Computers and Mathematics with Applications 74 (2017) 2089–2105

Contents lists available at ScienceDirect

Computers and Mathematics with Applications

journal homepage: www.elsevier.com/locate/camwa

# Regularity estimates and optimal finite element methods in $W_p^1$ on polygonal domains

Guanghao Jin [a], Young-Ju Lee [b], Hengguang Li [c,*]

[a] School of Computer Science & Software Engineering, Tianjin Polytechnic University, Tianjin, 300387, China
[b] Department of Mathematics, Texas State University, San Marcos, TX 78666, USA
[c] Department of Mathematics, Wayne State University, Detroit, MI 48202, USA

ARTICLE INFO

*Article history:*
Available online 6 March 2017

Dedicated to the Ninetieth Birthday of Professor Ivo Babuška

*Keywords:*
Regularity
Singular solution
Non-energy norm
Optimal finite element method

ABSTRACT

Consider the Poisson equation with the Dirichlet boundary condition on a bounded convex polygonal domain $\Omega \subset \mathbb{R}^2$. We investigate the finite element approximation of singular solutions that are due to the non-smoothness of the domain in the $W_p^1$ norm ($1 < p \leq \infty$). In particular, with analysis in weighted Sobolev spaces and weighted Hölder spaces, we provide *regularity requirements* on the given data and specific *parameter-selection criteria* for graded meshes, such that the resulting numerical approximation achieves the optimal convergence rate in $W_p^1$. Sample results from various numerical tests are provided to confirm the theory.



## 1. Introduction

Let $\Omega \subset \mathbb{R}^2$ be a bounded convex polygonal domain. We consider the Poisson equation with the Dirichlet boundary condition

$$-\Delta u = f \quad \text{in } \Omega, \qquad u = 0 \quad \text{on } \partial\Omega. \tag{1}$$

Given a function $f$ in $H^{-1}$ (the dual space of $H_0^1$), Eq. (1) has a unique $H^1$ solution $u$. It is well known that, due to the non-smoothness of the domain, the solution $u$ may be singular even if the data function $f$ is smooth. This lack of regularity can severely decrease the efficacy of the numerical approximation, and has been one of the major concerns in the computational community. Using continuous piecewise polynomials, the finite element solution to (1) is defined by a variational formulation and has a well-developed optimal convergence theory in the naturally-induced $H^1$ (energy) norm for smooth solutions [1,2]. In the presence of singular solutions, mesh grading techniques are widely used, such that the optimal $H^1$ energy-norm convergence rate can be recovered in the finite element method (see [3–9] and references therein). Beyond the energy norm, it is of both theoretical and practical importance [10–13] to investigate finite element approximations of singular solutions in the $W_p^1$ norm.

The $W_p^1$ analysis has a long history and early results can be traced back to 1970's [14–20]. In contrast to the case in the $H^1$ norm, the numerical solution does not inherit the stability in the Banach space $W_p^1$ ($p \neq 2$) from the variational formulation. Thus, extensive effort has been made on the stability analysis for the finite element solution in the $W_p^1$ norm. The analysis in these non-energy norms in general is technical, challenging, and requires additional geometric constraints on the mesh. In particular, the $W_p^1$ stability on *quasi-uniform* meshes can be found in [17]. These estimates in turn imply that the

* Corresponding author.
*E-mail addresses:* jinguanghao@tjpu.edu.cn (G. Jin), yjlee@txstate.edu (Y.-J. Lee), hli@math.wayne.edu (H. Li).

http://dx.doi.org/10.1016/j.camwa.2017.02.011

finite element approximation achieves the optimal convergence rate in $W_p^1$ when the solution is sufficiently smooth. Allowing mesh grading, error estimates in other non-energy norms are available in the literature. For example, see [21,22,18,19] for $L^\infty$ estimates on graded meshes for different elliptic problems. Recently, the $W_p^1$ stability of the finite element solution to Eq. (1) has been established on a class of graded meshes for possible singular solutions [11,13]. In spite of these developments, some critical questions remain open, including: [I] the regularity requirement on the data function $f$ ($f$ is assumed to be "sufficiently smooth" in the existing stability analysis in order for the solution to have the desired regularity. More sophisticated regularity analysis is needed for broader applications); [II] the specific construction of graded meshes for obtaining optimal numerical approximations in $W_p^1$ norms.

This paper is aiming at addressing these issues. Namely, we shall present regularity requirements on the given data $f$ and specific parameter-selection criteria for graded meshes, such that the resulting numerical approximation to Eq. (1) achieves the optimal convergence rate in $W_p^1$ norms for $1 < p \le \infty$, even when the solution is singular. The novelty of our approach lies in rigorous analysis in a family of weighted spaces: the weighted Sobolev space $\mathcal{K}_{\vec{\mu}}^{m,p}$ (Definition 2.1) and the weighted Hölder space $\mathcal{H}_{\vec{\mu}}^{m,\sigma}$ (Definition 2.3). Using these spaces, we are able to describe the full-regularity dependence of the solution on the data $f$ (Propositions 2.6 and 2.7). Then, the finite element error estimation is built upon these weighted regularity results and upon the intrinsic scaling property in the weighted space $\mathcal{K}_{\vec{\mu}}^{m,p}$.

To be more precise, we give a simple and explicit construction for a sequence of graded meshes $\mathcal{T}_n$. This construction is based on successive refinements of triangles according to a set of grading parameters. Denote by $S_n \subset H_0^1$ the finite element space associated with the mesh $\mathcal{T}_n$. Let $u_n \in S_n$ be the finite element solution. Then, we give smoothness requirements on $f$ and the range of grading parameters (Theorem 4.6), such that the following error estimate holds on $\mathcal{T}_n$:

$$\|u - u_n\|_{W_p^1(\Omega)} \le C\,\dim(S_n)^{-k/2}, \quad p \in (1, \infty], \tag{2}$$

where $\dim(S_n)$ and $k \ge 1$ are the dimension and the degree of the finite element space $S_n$, respectively, and $C > 0$ is independent of the mesh level. Namely, we are able to recover the approximation rate that is expected for smooth solutions. Note that we restrict our analysis on convex domains, because the stability of the Ritz projection [11,13] is available only on such domains for the time being. However, it is possible to extend our approach to non-convex domains under the condition that the corresponding stability result holds. Nevertheless, since $u \in W_p^m$ does not always hold for any $m$ and $p$ even on convex domains (Proposition 2.4), mesh grading is necessary to improve the finite element approximation to such singular solutions.

The rest of the paper is organized as follows. In Section 2, we introduce the weighted spaces $\mathcal{K}_{\vec{\mu}}^{m,p}$ and $\mathcal{H}_{\vec{\mu}}^{m,\sigma}$. In addition, we give full-regularity estimates for the solution of Eq. (1) in these spaces. In Section 3, we first define the graded meshes and the associated finite element methods. Then, we obtain a stability result that we shall need in the error analysis. In Section 4, with a detailed interpolation error estimate in the weighted space, we obtain our main result (Theorem 4.6) on the optimal finite element methods in the $W_p^1$ norm. In Section 5, we implement the proposed finite element algorithm for a model problem on various polygonal domains. We report the convergence rates of the linear finite element solution in the $W_p^1$ norm for different values of $p$. These numerical results verify the theoretical prediction and validate our parameter-selection criteria for graded meshes. In Section 6, we conclude the paper with some remarks.

Throughout the paper, by $A \simeq B$, we mean that there are constants $C_1 > 0$ and $C_2 > 0$, such that $C_1 A \le B \le C_2 A$. The generic constant $C > 0$ in our analysis below may be different at different occurrences. It will depend on the computational domain, but not on the functions involved in the estimates or the mesh level in the finite element algorithms.

## 2. Weighted spaces and regularity

In this section, we introduce function spaces for the analysis of Eq. (1); and establish regularity results for the solution in suitable weighted spaces.

### 2.1. Function spaces

For any $\omega \subset \Omega$, we use the standard notation $W_p^m(\omega)$ for the Sobolev space. Namely, for $m \ge 0$, the semi-norms and norms are

$$|v|_{W_p^m(\omega)} := \left(\sum_{|\alpha|=m} \int_\omega |\partial^\alpha v|^p dx\right)^{1/p}, \qquad \|v\|_{W_p^m(\omega)} := \left(\sum_{j\le m} |v|^p_{W_p^j(\omega)}\right)^{1/p}, \quad \text{for } 1 < p < \infty;$$

$$|v|_{W_\infty^m(\omega)} := \max_{|\alpha|=m}\big(\operatorname{ess\,sup}\{|\partial^\alpha v(x)|,\ x \in \omega\}\big), \qquad \|v\|_{W_\infty^m(\omega)} := \max_{j\le m}\big(|v|_{W_\infty^j(\omega)}\big),$$

where $\alpha = (\alpha_1, \alpha_2) \in \mathbb{Z}^2_{\ge 0}$ is the multi-index and $|\alpha| := \alpha_1 + \alpha_2$. In addition, given $\sigma \in (0, 1)$, recall that the Hölder space $C^{m,\sigma}(\omega)$ has the following norm

$$\|v\|_{C^{m,\sigma}(\omega)} := \sup_{x\in\omega} \sum_{|\alpha|\le m} |\partial^\alpha v| + \sum_{|\alpha|=m} \sup_{x,y\in\omega} \frac{|\partial^\alpha v(x) - \partial^\alpha v(y)|}{|x-y|^\sigma}.$$

The regularity of the solution to Eq. (1) depends on the given function $f$ and on the geometry of the domain $\Omega$. On a polygonal domain, the solution may not possess high-order derivatives in the Sobolev spaces, even when $f$ is smooth. We now introduce a class of weighted Sobolev spaces that shall give rise to sharp regularity descriptions for the singular solutions.

Recall the polygonal domain $\Omega$. Let $v_i$, $1 \le i \le l$, be the $i$th vertex of $\Omega$ and $\mathcal{V} := \{v_i\}_{i=1,\dots,l}$ be the vertex set. Denote by $r_i(x)$ be the distance function from $x \in \Omega$ to $v_i$. Let $\vec{\mu} := (\mu_1, \mu_2, \dots, \mu_l)$ be an $l$-dimensional vector. For a constant $c$, we denote $c \pm \vec{\mu} := (c \pm \mu_1, c \pm \mu_2, \dots, c \pm \mu_l)$. Then, we define the function

$$\rho(x) := \prod_{1 \le i \le l} r_i(x),$$

and its vector exponents

$$\rho^{c \pm \vec{\mu}}(x) := \prod_{1 \le i \le l} r_i(x)^{c \pm \mu_i} = \rho^c \prod_{1 \le i \le l} r_i(x)^{\pm \mu_i}.$$

Thus, we define the following weighted Sobolev space.

**Definition 2.1** (*Weighted Sobolev Spaces*)**.** For $\omega \subset \Omega$, the weighted Sobolev space is

$$\mathcal{K}^{m,p}_{\vec{\mu}}(\omega) := \{v,\ \rho^{|\alpha| - \vec{\mu}} \partial^\alpha v \in L^p(\omega) \text{ for all } |\alpha| \le m\}, \quad 1 < p \le \infty,$$

with the semi-norms and norms

$$|v|_{\mathcal{K}^{m,p}_{\vec{\mu}}(\omega)} := \left( \sum_{|\alpha|=m} \|\rho^{m-\vec{\mu}} \partial^\alpha v\|^p_{L^p(\omega)} \right)^{1/p}, \qquad \|v\|^2_{\mathcal{K}^{m,p}_{\vec{\mu}}(\omega)} := \left( \sum_{|\alpha| \le m} |v|^p_{\mathcal{K}^{|\alpha|,p}_{\vec{\mu}}(\omega)} \right)^{1/p}, \quad \text{for } 1 < p < \infty;$$

$$|v|_{\mathcal{K}^{m,\infty}_{\vec{\mu}}(\omega)} := \max_{|\alpha|=m} \left( \operatorname{ess\,sup}\{|\rho^{m-\vec{\mu}} \partial^\alpha v(x)|,\ x \in \omega\} \right), \qquad \|v\|_{\mathcal{K}^{m,\infty}_{\vec{\mu}}(\Omega)} := \max_{|\alpha| \le m} \left( |v|_{\mathcal{K}^{|\alpha|,\infty}_{\vec{\mu}}(\omega)} \right).$$

**Remark 2.2.** These weighted spaces are the by-products of the Mellin transform [23,24]. A special case of the space, $\mathcal{K}^{m,2}_{\vec{\mu}}$, is frequently used in the regularity analysis for elliptic equations with corner singularities. See [25–28,7] and references therein. We shall use the generalized version $\mathcal{K}^{m,p}_{\vec{\mu}}$ $(1 < p \le \infty)$ to handle the singular solution for analysis in the $W^1_p$ space. Note that the space $\mathcal{K}^{m,p}_{\vec{\mu}}$ has the following notable local property. Let $\omega_i \subset \Omega$ be a region within the neighborhood of the vertex $v_i$, which does not include other vertices. Then,

$$|v|_{\mathcal{K}^{m,p}_{\vec{\mu}}(\omega_i)} \simeq \left( \sum_{|\alpha|=m} \|r_i^{m-\mu_i} \partial^\alpha v\|^p_{L^p(\omega_i)} \right)^{1/p}, \quad 1 < p < \infty, \qquad |v|_{\mathcal{K}^{m,\infty}_{\vec{\mu}}(\omega_i)} \simeq \sum_{|\alpha|=m} \|r_i^{m-\mu_i} \partial^\alpha v\|_{L^\infty(\omega_i)}. \tag{3}$$

However, on a region $\omega \subset \Omega$ away from the vertex set $\mathcal{V}$, the weight function $\rho$ is bounded both above and below from zero. Therefore, the weighted space $\mathcal{K}^{m,p}_{\vec{\mu}}$ and the Sobolev space $W^m_p$ are equivalent. Namely, for $1 < p \le \infty$,

$$\|v\|_{\mathcal{K}^{m,p}_{\vec{\mu}}(\omega)} \simeq \|v\|_{W^m_p(\omega)}. \tag{4}$$

These local properties make it possible in $\mathcal{K}^{m,p}_{\vec{\mu}}$ to capture the singular behavior of the solution due to the non-smoothness of the domain.

In addition to the space $\mathcal{K}^{m,p}_{\vec{\mu}}$, we shall need the following weighted Hölder space [23] to obtain the regularity estimate for the case $p = \infty$.

**Definition 2.3** (*Weighted Hölder Spaces*)**.** Let $\sigma \in (0, 1)$. Then, for $\omega \subset \Omega$, the weighted Hölder space is

$$\mathcal{H}^{m,\sigma}_{\vec{\mu}}(\omega) := \left\{ v,\ \sup_{x \in \omega} \sum_{|\alpha| \le m} \rho^{|\alpha| - \sigma - \vec{\mu}} |\partial^\alpha v| + \sum_{|\alpha|=m} \sup_{x,y \in \omega} |x-y|^{-\sigma} |\rho^{m-\vec{\mu}} \partial^\alpha v(x) - \rho^{m-\vec{\mu}} \partial^\alpha v(y)| < \infty \right\},$$

with the norm

$$\|v\|_{\mathcal{H}^{m,\sigma}_{\vec{\mu}}(\omega)} := \sup_{x \in \omega} \sum_{|\alpha| \le m} \rho^{|\alpha| - \sigma - \vec{\mu}} |\partial^\alpha v| + \sum_{|\alpha|=m} \sup_{x,y \in \omega} \frac{|\rho^{m-\vec{\mu}} \partial^\alpha v(x) - \rho^{m-\vec{\mu}} \partial^\alpha v(y)|}{|x-y|^\sigma}.$$

### 2.2. Regularity estimates

Let $H_0^1(\Omega) \subset H^1(\Omega) := W_2^1(\Omega)$ be the subspace consisting of functions with zero trace on $\partial\Omega$. The variational solution $u \in H_0^1(\Omega)$ of Eq. (1) is

$$a(u, v) = \int_\Omega \nabla u \cdot \nabla v dx = \int_\Omega f v dx = (f, v), \quad \forall v \in H_0^1(\Omega). \tag{5}$$

By the Poincaré inequality, for any $f \in H^{-1}(\Omega)$, the solution $u \in H_0^1(\Omega)$ is well defined. However, on polygonal domains, it is known that the solution is not always smoother than $f$ in the Sobolev spaces (Section 2.7 in [29]):

**Proposition 2.4.** *Let $\chi$ be the largest interior angle of $\Omega$. The Laplace operator*

$$-\Delta : W_p^{m+2}(\Omega) \cap H_0^1(\Omega) \to W_p^m(\Omega), \quad m \geq 0,$$

*defines an isomorphism, provided that the parameter $p$ satisfies $1 < p < \eta_m$, where*

$$\begin{cases} \eta_m = \infty & \text{for } \pi/\chi \geq m+2; \\ \eta_m = \dfrac{2}{m+2-\pi/\chi} & \text{for } \pi/\chi < m+2. \end{cases}$$

**Remark 2.5.** The lack of regularity in $W_p^m$ for large values of $m$ and $p$ is due to the fact that near a vertex $v_i \in \mathcal{V}$ of the domain, the solution has the following expansion

$$u = u_S + u_R = \sum_{s,t} c_{s,t} \psi r^s \ln^t r + u_R,$$

where $u_R \in W_p^{m+2}(\Omega)$ is the smoother component, $\psi$ is a smooth function, and $r$ is the distance to $v_i$. The constants $c_{s,t} \in \mathbb{R}$ and $s, t \in \mathbb{R}_+ \cup \{0\}$ depend on the local geometry of the vertex. Therefore, the singular component $u_S = \sum_{s,t} c_{s,t} \psi r^s \ln^t r$ may not be in $W_p^{m+2}(\Omega)$, regardless of the smoothness of right hand side $f$.

By contrast, we have the following full-regularity estimates in weighted spaces for solutions with such corner singularities.

**Proposition 2.6.** *Let $\chi_i$, $1 \leq i \leq l$, be the interior angle associated with the ith vertex $v_i \in \mathcal{V}$ and $\vec{a} := (a_1, a_2, \ldots, a_l)$. For $1 < p < \infty$, define $\eta_i := \pi/\chi_i - 1 + 2/p$. Then, for any $0 \leq a_i < \eta_i$, if $f \in \mathcal{K}_{-\vec{1}}^{0,2}(\Omega) \cap \mathcal{K}_{\vec{a}-\vec{1}}^{m,p}(\Omega)$, $m \geq 0$, the variational solution of Eq. (1) satisfies*

$$\|u\|_{\mathcal{K}_{\vec{a}+\vec{1}}^{m+2,p}(\Omega)} \leq C\|f\|_{\mathcal{K}_{\vec{a}-\vec{1}}^{m,p}(\Omega)},$$

*where $\vec{1} = (1, 1, \ldots, 1)$ is an l-dimensional constant vector.*

**Proof.** Based on Lemma 3.5 in [7], $H_0^1(\Omega)$ and $\mathcal{K}_1^{1,2}(\Omega) \cap \{v|_{\partial\Omega} = 0\}$ are the same space. Thus, for $f \in \mathcal{K}_{-1}^{0,2}(\Omega)$, by the regularity estimate in weighted spaces (Theorem 3.3 in [7]), we first have $u \in \mathcal{K}_1^{2,2}(\Omega)$.

Then, using a partition of unity, we can apply the localization argument for the solution in each neighborhood $\omega_i$ of the vertex $v_i$ and in an interior subdomain $\omega$ away from the vertices. Near a vertex $v_i$, the eigenvalues of the operator pencil associated with the Laplace operator in Eq. (1) are $\pm k\pi/\chi_i$, $k \in \mathbb{Z}_+$ [5,30]. Note that the space $V_\beta^{m,p}$ in [30] is the same as $\mathcal{K}_{\vec{\mu}}^{m,p}$ when $m - \beta = \mu_i$. Therefore, in the neighborhood $\omega_i$ of the vertex $v_i$, by Corollary 1.2.7 in [30] and the norm equivalence (3), we have

$$\|u\|_{\mathcal{K}_{\vec{a}+\vec{1}}^{m+2,p}(\omega_i)} \leq C\|f\|_{\mathcal{K}_{\vec{a}-\vec{1}}^{m,p}(\omega_i)}$$

as long as $|a_i + 1 - 2/p| < \pi/\chi_i$. In the interior subdomain $\omega$, we can use Theorem 9.19 in [31] and the norm equivalence (4) to obtain

$$\|u\|_{\mathcal{K}_{\vec{a}+\vec{1}}^{m+2,p}(\omega)} \simeq \|u\|_{W_p^{m+2}(\omega)} \leq C\|f\|_{W_p^m(\omega)} \simeq \|f\|_{\mathcal{K}_{\vec{a}-\vec{1}}^{m,p}(\omega)}.$$

Hence, combining all the local estimates, we have for $1 < p < \infty$,

$$\|u\|_{\mathcal{K}_{\vec{a}+\vec{1}}^{m+2,p}(\Omega)} \leq C\|f\|_{\mathcal{K}_{\vec{a}-\vec{1}}^{m,p}(\Omega)}, \quad \text{for } -\frac{\pi}{\chi_i} - 1 + \frac{2}{p} < a_i < \frac{\pi}{\chi_i} - 1 + \frac{2}{p}.$$

Since $\Omega$ is convex, $\chi_i < \pi$, and therefore $-\frac{\pi}{\chi_i} - 1 + \frac{2}{p} < 0$. Thus, the estimate above holds for $0 \leq a_i < \eta_i$, which completes the proof. $\square$

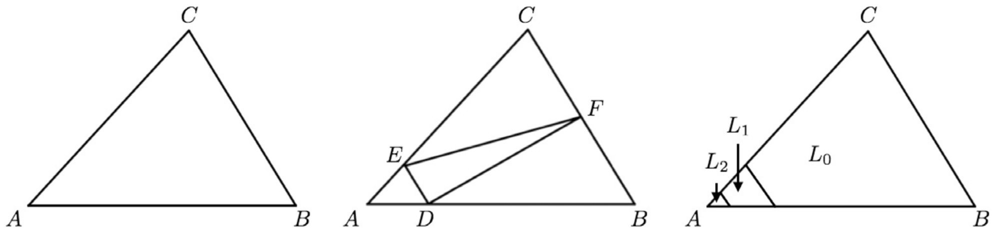


**Fig. 1.** Graded triangulations and mesh layers (left–right): an initial triangle with $A \in \mathcal{V}$ and $B, C \notin \mathcal{V}$; one graded refinement to $A$, $\kappa_A = \frac{|AD|}{|AB|} = \frac{|AE|}{|AC|} = \frac{|DE|}{|BC|}$; three mesh layers resulted by two consecutive graded refinements toward $A$.

In order to obtain the regularity estimate for $p = \infty$, we use the weighted Hölder space in Definition 2.3. The following result can be found in Section 8.7.1 of [23], in which the space $N^{m,\sigma}_{\vec{\beta}}$ is the same as $\mathcal{H}^{m,\sigma}_{\vec{\mu}}$ for $\mu_i = m - \beta_i$.

**Proposition 2.7.** *Let $\chi_i$, $1 \le i \le l$, be the interior angle associated with the ith vertex $v_i$ and $\vec{a} := (a_1, a_2, \dots, a_l)$. Let $M := \min_{1\le i\le l}(\pi/\chi_i - 1)$. Note that $M > 0$ on the convex polygonal domain. For any $\sigma \in (0, \min(1, M))$, define $\eta_i := \pi/\chi_i - 1 - \sigma$. Then, for $0 \le a_i < \eta_i$, if $f \in \mathcal{H}^{m,\sigma}_{\vec{a}-\vec{1}}(\Omega)$, $m \ge 0$, the variational solution of Eq. (1) satisfies*

$$\|u\|_{\mathcal{H}^{m+2,\sigma}_{\vec{a}+\vec{1}}(\Omega)} \le C\|f\|_{\mathcal{H}^{m,\sigma}_{\vec{a}-\vec{1}}(\Omega)}.$$

Note that by Definitions 2.1 and 2.3, for any $v \in \mathcal{H}^{m,\sigma}_{\vec{\mu}}(\Omega)$, we have

$$\|v\|_{\mathcal{K}^{m,\infty}_{\vec{\mu}}(\Omega)} \le C\|v\|_{\mathcal{H}^{m,\sigma}_{\vec{\mu}}(\Omega)}. \tag{6}$$

Therefore, by (6) and Proposition 2.7, we obtain the following estimate in $\mathcal{K}^{m,\infty}_{\vec{\mu}}(\Omega)$.

**Corollary 2.8.** *Recall the parameters $\chi_i$, $\sigma$, $\eta_i$, and $a_i$ from Proposition 2.7. Then, for $f \in \mathcal{H}^{m,\sigma}_{\vec{a}-\vec{1}}(\Omega)$, $m \ge 0$, the variational solution of Eq. (1) satisfies*

$$\|u\|_{\mathcal{K}^{m+2,\infty}_{\vec{a}+\vec{1}}(\Omega)} \le C\|f\|_{\mathcal{H}^{m,\sigma}_{\vec{a}-\vec{1}}(\Omega)}.$$

**Remark 2.9.** The regularity estimates in Proposition 2.6 and Corollary 2.8 imply high-order smoothness of the solution $u$ in weighted Sobolev spaces $\mathcal{K}^{m,p}_{\vec{\mu}}(\Omega)$, provided that the given function $f$ is reasonably smooth. For example, for $0 \le a_i \le 1$, one can see $W^m_p(\Omega) \subset \mathcal{K}^{m,p}_{\vec{a}-\vec{1}}(\Omega)$ for $1 < p < \infty$; and for $0 \le a_i \le 1 - \sigma$, we have $C^{m,\sigma}(\Omega) \subset \mathcal{H}^{m,\sigma}_{\vec{a}-\vec{1}}(\Omega)$.

## 3. Finite element methods

In this section, we describe the construction of a class of graded meshes and the associated finite element methods. In addition, we discuss the geometric properties of the mesh and the stability properties of the numerical algorithm, both of which are critical for our further analysis.

**Definition 3.1** (*Graded Meshes*)**.** Let $\mathcal{T}$ be a triangulation of $\Omega$ whose vertices include $\mathcal{V}$, such that no triangle in $\mathcal{T}$ has more than one of its vertices in $\mathcal{V}$. Define the vector $\vec{\kappa} = (\kappa_1, \kappa_2, \dots, \kappa_l)$, for $\kappa_i \in (0, 1/2]$. Then, *a $\vec{\kappa}$ refinement of $\mathcal{T}$*, denoted by $\vec{\kappa}(\mathcal{T})$, is obtained by dividing each edge $AB$ of $\mathcal{T}$ in two parts as follows:

- If neither $A$ nor $B$ is in $\mathcal{V}$, then we divide $AB$ into two equal parts.
- Otherwise, if $A = v_i \in \mathcal{V}$, we divide $AB$ into $AD$ and $DB$ such that $|AD| = \kappa_i|AB|$.

This will divide each triangle of $\mathcal{T}$ into four triangles (Fig. 1). Given an initial triangulation $\mathcal{T}_0$, the associated family of graded triangulations $\{\mathcal{T}_j : j \ge 0\}$ is defined recursively, $\mathcal{T}_{j+1} = \vec{\kappa}(\mathcal{T}_j)$.

Let $S_n \subset H^1_0(\Omega)$, $n \ge 0$, be the Lagrange finite element space of degree $k \ge 1$ associated with the graded triangulation $\mathcal{T}_n$. Namely,

$$S_n = \{v \in C(\Omega),\ v|_T \in \mathcal{P}_k,\ \text{for any triangle } T \in \mathcal{T}_n\},$$

where $\mathcal{P}_k$ is the space of polynomials of degree $\le k$. Then, the finite element solution $u_n \in S_n$ for Eq. (1) satisfies

$$a(u_n, v_n) = (f, v_n), \quad \forall v_n \in S_n, \tag{7}$$

where $a(\cdot,\cdot)$ is the bilinear form defined in (5).

**Remark 3.2.** Note that successive graded refinements (Definition 3.1) for a triangle $T \in \mathcal{T}_0$ generate child triangles within at most four similarity classes. Therefore, the triangles in $\mathcal{T}_n$ is within at most $4N_0$ similarity classes, where $N_0$ is the number of initial triangles in $\mathcal{T}_0$. Thus, $\mathcal{T}_n$ consists of shape-regular triangles.

**Remark 3.3.** In the construction of graded meshes (Definition 3.1), the value of $\kappa_i$ controls the mesh density near the vertex $v_i$. When $\kappa_i = 1/2$, the successive refinements lead to a quasi-uniform mesh in the neighborhood of $v_i$ (Fig. 2). In the presence of singular solutions, this graded mesh, when an appropriate grading parameter $\vec{\kappa}$ is chosen, has been successful in recovering the optimal rate of convergence of the finite element solution in the energy norm [5,7]. The novelty of our results is the development of explicit graded meshes, on which the optimal convergence rate can be achieved for the finite element solution in the $W^1_p$ norm.

We now derive the following stability result for the finite element solution on these graded meshes.

**Theorem 3.4.** *Recall the graded mesh $\mathcal{T}_n$ from Definition 3.1 and the finite element solution $u_n$ from (7). Let $f$ be given as in Proposition 2.6 for $1 < p < \infty$ and be given as in Proposition 2.7 for $p = \infty$. Then, for $n$ sufficiently large and $m \geq 0$, we have*

$$\|u_n\|_{W^1_p(\Omega)} \leq C\|u\|_{W^1_p(\Omega)} \leq C\|f\|_{\mathcal{K}^{m,p}_{\vec{a}-\vec{1}}(\Omega)}, \quad 1 < p < \infty \tag{8}$$

*and*

$$\|u_n\|_{W^1_\infty(\Omega)} \leq C\|u\|_{W^1_\infty(\Omega)} \leq C\|f\|_{\mathcal{H}^{m,\sigma}_{\vec{a}-\vec{1}}(\Omega)}, \tag{9}$$

*where $C$ is independent of the mesh level $n$.*

**Proof.** Under the assumption that the solution $u \in W^1_p(\Omega)$ with $1 < p \leq \infty$, the stability of the Ritz projection on graded meshes is proved (see [11] and Theorem 5.5 in [13]) for $n$ sufficiently large

$$\|u_n\|_{W^1_p(\Omega)} \leq C\|u\|_{W^1_p(\Omega)}.$$

Therefore, we only need to show the second inequality in (8) and (9). Namely, $u \in W^1_p(\Omega)$ provided that the function $f$ is as described.

Recall that in both Propositions 2.6 and 2.7, $a_i \geq 0$ and $m \geq 0$. Then, for $1 < p < \infty$, by the definition of the weighted space and Proposition 2.6, we have

$$\|u\|_{W^1_p(\Omega)} \leq C\|u\|_{\mathcal{K}^{1,p}_{\vec{a}+\vec{1}}(\Omega)} \leq C\|f\|_{\mathcal{K}^{m,p}_{\vec{a}-\vec{1}}(\Omega)}.$$

For $p = \infty$, by the definition of the weighted space and Corollary 2.8, we have

$$\|u\|_{W^1_\infty(\Omega)} \leq C\|u\|_{\mathcal{K}^{1,\infty}_{\vec{a}+\vec{1}}(\Omega)} \leq C\|f\|_{\mathcal{H}^{m,\sigma}_{\vec{a}-\vec{1}}(\Omega)}.$$

Hence, the proof is completed. □

**Corollary 3.5.** *For $1 < p \leq \infty$ and $n$ sufficiently large, let $f$ be given as in Theorem 3.4. Then, we have*

$$\|u - u_n\|_{W^1_p(\Omega)} \leq C \inf_{v \in S_n} \|u - v\|_{W^1_p(\Omega)}. \tag{10}$$

**Proof.** By Theorem 3.4, for the given $f$, $u \in W^1_p(\Omega)$ for $1 < p \leq \infty$. Therefore, for any $v \in S_n$, we have

$$\|u - u_n\|_{W^1_p(\Omega)} \leq \|u - v\|_{W^1_p(\Omega)} + \|v - u_n\|_{W^1_p(\Omega)} \leq C\|u - v\|_{W^1_p(\Omega)}.$$

This completes the proof. □

**Remark 3.6.** Corollary 3.5 generalizes the Céa Theorem in the $H^1$ error analysis. Namely, the finite element solution is comparable to the best approximation in the $W^1_p$ norm on the graded mesh. Based on Theorem 3.4, the constant $C$ in (10) is independent of the mesh level $n$ and depends on the grading parameter $\vec{\kappa}$. We, however, note that $C$ is bounded for a sequence of graded meshes $\mathcal{T}_j, j \leq n$, once $\vec{\kappa}$ is fixed. These results allow us to focus on interpolation error estimates in these non-energy norms, and in turn to improve the accuracy of the numerical solution on graded meshes (see Section 4).

A close examination of the graded mesh leads to the following definition of mesh layers that are associated with graded refinements toward the vertices.

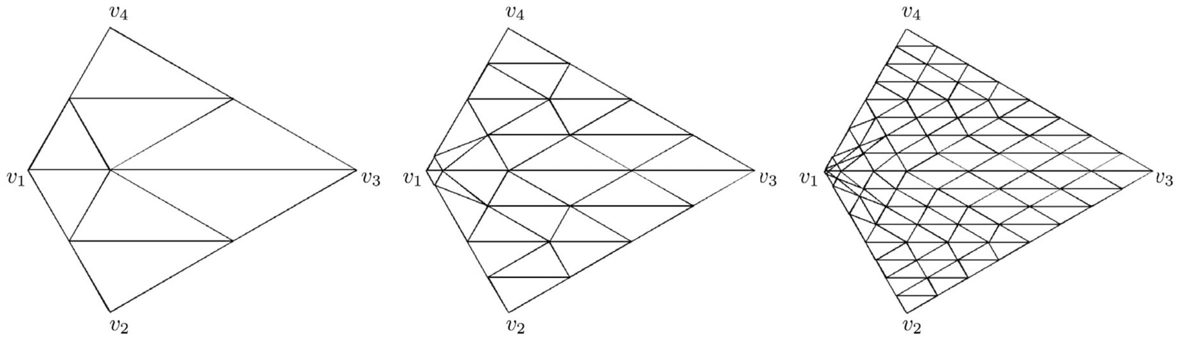


**Fig. 2.** Three consecutive graded refinements of a polygonal domain with $\vec{\kappa} = (0.2, 0.5, 0.5, 0.5)$ (left–right): $\mathcal{T}_0$, the initial triangulation; $\mathcal{T}_1$, the mesh after one refinement; $\mathcal{T}_2$, the mesh after two refinements.

**Definition 3.7** (*Mesh Layers*)**.** Recall from Definition 3.1 that the triangulation $\mathcal{T}_j$, $0 \leq j \leq n$, is obtained after $j$ successive graded refinements of $\mathcal{T}_0$ with parameter $\vec{\kappa}$. Let $\mathbb{T}_{i,j} \subset \mathcal{T}_j$, $1 \leq i \leq l$, be the union of (closed) triangles in $\mathcal{T}_j$ having $v_i \in \mathcal{V}$ as a vertex. Namely, $\mathbb{T}_{i,j}$ is the immediate neighborhood of $v_i$ in $\mathcal{T}_j$. Define the regions near $v_i$, resulting from the graded refinement

$$L_{i,j} = \mathbb{T}_{i,j} \setminus \mathbb{T}_{i,j+1}, \quad \text{for } 0 \leq j < n, \quad \text{and} \quad L_{i,n} = \mathbb{T}_{i,n}.$$

Then, we denote the $j$th layer $L_j$, $0 \leq j \leq n$, of the mesh $\mathcal{T}_n$ by

$$L_j = \cup_{1 \leq i \leq l} L_{i,j}.$$

See Fig. 1 for an illustration of mesh layers.

**Remark 3.8.** Let $\Omega_0 := \Omega \setminus \cup_i \mathbb{T}_{i,0}$. It is apparent that $\Omega = \Omega_0 \cup (\cup_{0 \leq j \leq n} L_j)$. Based on Definition 3.1, on $\mathcal{T}_n$, the diameter of the triangles in $\Omega_0$ is

$$h \simeq 2^{-n}; \tag{11}$$

the mesh size in each layer $L_{i,j}$ is

$$h_{i,j} \simeq \kappa_i^j 2^{j-n}; \tag{12}$$

and the dimension of the finite element space, determined by the number of triangles in $\mathcal{T}_n$ is

$$\dim(S_n) \simeq 4^n. \tag{13}$$

In addition, since $L_{i,j}$ is in the neighborhood of $v_i$, by Definitions 2.1 and 3.1, the weight function $\rho$ and the distance function $r_i$ satisfy

$$\rho|_{L_{i,j}} \simeq r_i|_{L_{i,j}} \simeq \kappa_i^j, \quad \text{for } 0 \leq j < n; \quad \text{and} \quad \rho|_{L_{i,n}} \simeq r_i|_{L_{i,n}} \leq C\kappa_i^n. \tag{14}$$

## 4. Error analysis and optimal meshes

In this section, we first investigate the interpolation error in the $W_p^1$ norm on graded meshes. Then, we summarize the main results in Theorem 4.6, where we provide the regularity requirement for the function $f$ and the selection criteria for the grading parameter $\vec{\kappa}$, such that the associated finite element method approximates the solution $u$ of Eq. (1) with the optimal rate in the $W_p^1$ norm.

Recall that $k \geq 1$ is the degree of the Lagrange finite element space $S_n$ associated with the triangulation $\mathcal{T}_n$ (Definition 3.1) with a grading parameter $\vec{\kappa}$. In view of (10), we shall obtain the finite element approximation error by analyzing the interpolation error.

Let $f$ be a function, such that $f \in \mathcal{K}^{0,2}_{-\vec{1}}(\Omega) \cap \mathcal{K}^{k-1,p}_{\vec{a}-\vec{1}}(\Omega)$ if $1 < p < \infty$ and $f \in \mathcal{H}^{k-1,\sigma}_{\vec{a}-\vec{1}}(\Omega)$ if $p = \infty$. Thus, for the values of $\vec{a}$ and $\sigma$ given in Propositions 2.6 and 2.7, the solution of Eq. (1) satisfies

$$u \in \mathcal{K}^{k+1,p}_{\vec{a}+\vec{1}}(\Omega), \quad 1 < p \leq \infty. \tag{15}$$

Thus, by the equivalence of norms (4) and the Sobolev embedding Theorem, $u$ is continuous in any interior region of the domain $\Omega$ that is away from the vertex $\mathcal{V}$. Note that by the definitions of the weighted spaces, $\mathcal{H}^{k-1,\sigma}_{\vec{a}-\vec{1}}(\Omega) \subset \mathcal{K}^{0,2}_{-\vec{1}}(\Omega)$. Therefore, in both cases ($1 < p < \infty$ and $p = \infty$), $f \in \mathcal{K}^{0,2}_{-\vec{1}}(\Omega)$. This implies $u \in \mathcal{K}^{2,2}_{\vec{1}}(\Omega)$ (Proposition 2.6). It was shown

(Lemma 4.7 in [32]) that the discontinuities of $u \in \mathcal{K}^{2,2}_{\vec{1}}(\Omega)$ at $\mathcal{V}$ are removable and $u \to 0$ when approaching the vertices. Hence, $u$ can be regarded as a continuous function on $\bar{\Omega}$ and $u(v_i) = 0$ for any $v_i \in \mathcal{V}$.

Now, we recall a general approximation result [1,2].

**Lemma 4.1.** *For a polygonal domain $G \subset \mathbb{R}^2$, let $\mathcal{T}$ be a quasi-uniform triangulation of $G$ with mesh size $h$. Let $S$ be the Lagrange finite element space of degree $k \geq 1$ associated with $\mathcal{T}$. For any $v \in W^{k+1}_p(G)$, $1 < p \leq \infty$, let $v_I \in S$ be its nodal interpolation. Then,*

$$\|v - v_I\|_{W^1_p(G)} \leq Ch^k |v|_{W^{k+1}_p(G)}$$

*where $C > 0$ is independent of $h$ and $v$.*

In view of (15) and the above arguments on its continuity, let $u_I \in S_n$ be the nodal interpolation of $u$. Recall the mesh layers $L_{i,j}$ from Definition 3.7. Then, we estimate the interpolation error in three regions for $u \in \mathcal{K}^{k+1,p}_{\vec{a}+\vec{1}}(\Omega)$: (I) $\Omega_0 := \Omega \setminus \cup_{i,j} L_{i,j}$; (II) $L_{i,j}$ for $0 \leq j < n$; and (III) $L_{i,n}$. In particular, on $\Omega_0$, we have the following.

**Lemma 4.2.** *Let $\mathcal{T}_n$ be the mesh given in Definition 3.1. On $\Omega_0$, recall the mesh size $h \simeq 2^{-n}$ from (11). Then,*

$$\|u - u_I\|_{W^1_p(\Omega_0)} \leq Ch^k \|u\|_{\mathcal{K}^{k+1,p}_{\vec{a}+\vec{1}}(\Omega_0)}, \quad 1 < p \leq \infty,$$

*where $C > 0$ is independent of $h$ and $u$.*

**Proof.** Since $\Omega_0$ is away from the vertex set $\mathcal{V}$, by (4), $\mathcal{K}^{k+1,p}_{\vec{a}+\vec{1}}$ and $W^{k+1}_p$ are equivalent on $\Omega_0$. Then, using the estimates in Lemma 4.1, we have

$$\|u - u_I\|_{W^1_p(\Omega_0)} \leq Ch^k \|u\|_{W^{k+1}_p(\Omega_0)} \leq Ch^k \|u\|_{\mathcal{K}^{k+1,p}_{\vec{a}+\vec{1}}(\Omega_0)}.$$

This completes the proof. $\square$

To carry out the error analysis on $L_{i,j}$, we need the following result regarding the dilation property in the weighted space. Recall the grading parameter $0 < \kappa_i \leq 1/2$ for the layer $L_{i,j}$. We consider a new coordinate system that is a simple translation of the old $xy$-coordinate system with the vertex $v_i$ now at the origin of the new coordinate system. For $0 \leq j \leq n$, we define the region with dilation

$$L'_{i,j} := \kappa_i^{-j} L_{i,j}; \tag{16}$$

and the dilation of a function $v$ on $L_{i,j}$ in the new coordinate system

$$v'(x, y) := v(\kappa_i^j x, \kappa_i^j y), \quad \forall (x, y) \in L'_{i,j}. \tag{17}$$

This definition makes sense, since $v_i$ is the origin in the new coordinate system. Then, we have the following lemma.

**Lemma 4.3.** *Recall the distance function $r_i$ to the vertex $v_i$. Then, for $m \geq 0$, if $v \in \mathcal{K}^{m,p}_{\vec{\mu}}(L_{i,j})$, $1 < p < \infty$, we have*

$$\sum_{|\alpha| \leq m} \|r_i^{|\alpha|-\mu_i} \partial^\alpha v\|^p_{L^p(L_{i,j})} = \kappa_i^{j(2-p\mu_i)} \sum_{|\alpha| \leq m} \|r_i^{|\alpha|-\mu_i} \partial^\alpha v'\|^p_{L^p(L'_{i,j})}; \tag{18}$$

*if $v \in \mathcal{K}^{m,\infty}_{\vec{\mu}}(L_{i,j})$, we have*

$$\sum_{|\alpha| \leq m} \|r_i^{|\alpha|-\mu_i} \partial^\alpha v\|_{L^\infty(L_{i,j})} = \kappa_i^{-j\mu_i} \sum_{|\alpha| \leq m} \|r_i^{|\alpha|-\mu_i} \partial^\alpha v'\|_{L^\infty(L'_{i,j})}, \tag{19}$$

*where $0 \leq j \leq n$.*

**Proof.** Since $L_{i,j}$ is in the neighborhood of the vertex $v_i$, the norm of the space $\mathcal{K}^{m,p}_{\vec{\mu}}(L_{i,j})$ has an equivalent expression shown in (3). Thus, for $v \in \mathcal{K}^{m,p}_{\vec{\mu}}(L_{i,j})$, $1 < p \leq \infty$, the left-hand-side terms in (18) and (19) are valid (finite).

For $(x, y) \in L'_{i,j}$, let $w = \kappa_i^j x$ and $z = \kappa_i^j y$. Then, by (16), $(w, z) \in L_{i,j}$. Thus, for the distance function $r_i$, we have $r_i(x, y) = \kappa_i^{-j} r_i(w, z)$. Therefore, for $1 < p < \infty$, we have

$$\begin{aligned}
\sum_{|\alpha| \leq m} \|r_i^{|\alpha|-\mu_i} \partial^\alpha v'\|^p_{L^p(L'_{i,j})} &= \sum_{|\alpha| \leq m} \int_{L'_{i,j}} |r_i^{|\alpha|-\mu_i}(x, y) \partial_x^{\alpha_1} \partial_y^{\alpha_2} v'(x, y)|^p dxdy \\
&= \sum_{|\alpha| \leq m} \int_{L_{i,j}} |\kappa_i^{j(\mu_i-|\alpha|)} r_i^{|\alpha|-\mu_i}(w, z) \kappa_i^{j|\alpha|} \partial_w^{\alpha_1} \partial_z^{\alpha_2} v(w, z)|^p \kappa_i^{-2j} dwdz
\end{aligned}$$

$$= \kappa_i^{j(p\mu_i-2)} \sum_{|\alpha|\le m} \int_{L_{i,j}} |r_i^{|\alpha|-\mu_i}(w,z)\partial_w^{\alpha_1}\partial_z^{\alpha_2} v(w,z)|^p dwdz$$
$$= \kappa_i^{j(p\mu_i-2)} \sum_{|\alpha|\le m} \|r_i^{|\alpha|-\mu_i}\partial^\alpha v\|^p_{L^p(L_{i,j})}.$$

This proves (18). For (19), we similarly have

$$\begin{aligned}\sum_{|\alpha|\le m} \|r_i^{|\alpha|-\mu_i}\partial^\alpha v'\|_{L^\infty(L'_{i,j})} &= \sum_{|\alpha|\le m} \|r_i^{|\alpha|-\mu_i}(x,y)\partial_x^{\alpha_1}\partial_y^{\alpha_2} v'(x,y)\|_{L^\infty(L'_{i,j})}\\ &= \sum_{|\alpha|\le m} \|\kappa_i^{j(\mu_i-|\alpha|)} r_i^{|\alpha|-\mu_i}(w,z)\kappa_i^{j|\alpha|}\partial_w^{\alpha_1}\partial_z^{\alpha_2} v(w,z)\|_{L^\infty(L_{i,j})}\\ &= \kappa_i^{j\mu_i} \sum_{|\alpha|\le m} \|r_i^{|\alpha|-\mu_i}\partial^\alpha v\|_{L^\infty(L_{i,j})},\end{aligned}$$

which completes the proof. □

Then, we give the error estimates on the mesh layers $L_{i,j}$ for $0 \le j < n$.

**Lemma 4.4.** *Let $\mathcal{T}_n$ be the mesh given in Definition 3.1. Then, for $0 \le j < n$, $1 < p \le \infty$, and $a_i > 0$, we have*

$$\|u-u_I\|_{W_p^1(L_{i,j})} \le C\kappa_i^{ja_i} 2^{k(j-n)} \|u\|_{\mathcal{K}^{k+1,p}_{\vec{a}+\vec{1}}(L_{i,j})},$$

*where $C > 0$ is independent of $j$ and $u$.*

**Proof.** By the definition of the weighted space (Definition 2.1), we first have

$$\|u-u_I\|_{W_p^1(L_{i,j})} \le C\|u-u_I\|_{\mathcal{K}^{1,p}_{\vec{1}}(L_{i,j})}.$$

Note that by the dilation (16), the weight function $\rho \simeq r_i \simeq 1$ on $L'_{i,j}$. Therefore, the $\mathcal{K}^{m,p}_{\vec{\mu}}$ norm and the $W_p^m$ norm are equivalent on $L'_{i,j}$. Recall the mesh size $h_{i,j} \simeq \kappa_i^j 2^{j-n}$ on $L_{i,j}$ from (12). Then, by the estimates in (3), (18), Lemma 4.1, and (14), for $1 < p < \infty$, we have

$$\begin{aligned}\|u-u_I\|^p_{W_p^1(L_{i,j})} &\le C\|u-u_I\|^p_{\mathcal{K}^{1,p}_{\vec{1}}(L_{i,j})} \le C\sum_{|\alpha|\le 1}\|r_i^{|\alpha|-1}\partial^\alpha(u-u_I)\|^p_{L^p(L_{i,j})}\\ &= C\kappa_i^{j(2-p)}\sum_{|\alpha|\le 1}\|r_i^{|\alpha|-1}\partial^\alpha(u'-\mathcal{I}u')\|^p_{L^p(L'_{i,j})} \le C\kappa_i^{j(2-p)}\|u'-\mathcal{I}u'\|^p_{W_p^1(L'_{i,j})}\\ &\le C\kappa_i^{j(2-p)}(h_{i,j}\kappa_i^{-j})^{pk}\|u'\|^p_{W_p^{k+1}(L'_{i,j})} \le C\kappa_i^{j(2-p)}(h_{i,j}\kappa_i^{-j})^{pk}\|u'\|^p_{\mathcal{K}^{k+1,p}_{\vec{1}}(L'_{i,j})}\\ &\le C(h_{i,j}\kappa_i^{-j})^{pk}\|u\|^p_{\mathcal{K}^{k+1,p}_{\vec{1}}(L_{i,j})} \le C(h_{i,j}\kappa_i^{-j})^{pk}\sum_{|\alpha|\le k+1}\|r_i^{|\alpha|-1}\partial^\alpha u\|^p_{L^p(L_{i,j})}\\ &\le C\kappa_i^{pja_i}(h_{i,j}\kappa_i^{-j})^{pk}\sum_{|\alpha|\le k+1}\|r_i^{|\alpha|-1-a_i}\partial^\alpha u\|^p_{L^p(L_{i,j})} \le C\kappa_i^{pja_i}(h_{i,j}\kappa_i^{-j})^{pk}\|u\|^p_{\mathcal{K}^{k+1,p}_{\vec{a}+\vec{1}}(L_{i,j})}\\ &\le C\kappa_i^{pja_i}2^{pk(j-n)}\|u\|^p_{\mathcal{K}^{k+1,p}_{\vec{a}+\vec{1}}(L_{i,j})}.\end{aligned}$$

For $p=\infty$, by the estimates in (3), (19), Lemma 4.1, (14), and (12), we have

$$\begin{aligned}\|u-u_I\|_{W_\infty^1(L_{i,j})} &\le C\|u-u_I\|_{\mathcal{K}^{1,\infty}_{\vec{1}}(L_{i,j})} \le C\sum_{|\alpha|\le 1}\|r_i^{|\alpha|-1}\partial^\alpha(u-u_I)\|_{L^\infty(L_{i,j})}\\ &= C\kappa_i^{-j}\sum_{|\alpha|\le 1}\|r_i^{|\alpha|-1}\partial^\alpha(u'-\mathcal{I}u')\|_{L^\infty(L'_{i,j})} \le C\kappa_i^{-j}\|u'-\mathcal{I}u'\|_{W_\infty^1(L'_{i,j})}\\ &\le C\kappa_i^{-j}(h_{i,j}\kappa_i^{-j})^{k}\|u'\|_{W_\infty^{k+1}(L'_{i,j})} \le C\kappa_i^{-j}(h_{i,j}\kappa_i^{-j})^{k}\|u'\|_{\mathcal{K}^{k+1,\infty}_{\vec{1}}(L'_{i,j})}\\ &\le C(h_{i,j}\kappa_i^{-j})^{k}\|u\|_{\mathcal{K}^{k+1,\infty}_{\vec{1}}(L_{i,j})} \le C(h_{i,j}\kappa_i^{-j})^{k}\sum_{|\alpha|\le k+1}\|r_i^{|\alpha|-1}\partial^\alpha u\|_{L^\infty(L_{i,j})}\\ &\le C\kappa_i^{ja_i}(h_{i,j}\kappa_i^{-j})^{k}\sum_{|\alpha|\le k+1}\|r_i^{|\alpha|-1-a_i}\partial^\alpha u\|_{L^\infty(L_{i,j})} \le C\kappa_i^{ja_i}(h_{i,j}\kappa_i^{-j})^{k}\|u\|_{\mathcal{K}^{k+1,\infty}_{\vec{a}+\vec{1}}(L_{i,j})}\\ &\le C\kappa_i^{ja_i}2^{k(j-n)}\|u\|_{\mathcal{K}^{k+1,\infty}_{\vec{a}+\vec{1}}(L_{i,j})}.\end{aligned}$$

Thus, the proof is completed. □

Now, we are ready to analyze the interpolation error on the last layer $L_{i,n}$.

**Lemma 4.5.** *Let $\mathcal{T}_n$ be the mesh given in Definition 3.1. Then, for $1 < p \leq \infty$ and $a_i > 0$, we have*

$$\|u - u_I\|_{W^1_p(L_{i,n})} \leq C\kappa_i^{na_i}\|u\|_{\mathcal{K}^{k+1,p}_{\vec{a}+\vec{1}}(L_{i,n})},$$

*where $C > 0$ is independent of $n$ and $u$.*

**Proof.** Let $u'(x, y) = u(\kappa_i^n x, \kappa_i^n y)$ be the dilation (17) of $u$ with $v_i$ as the origin. Then, $u' \in \mathcal{K}^{k+1,p}_{\vec{a}+\vec{1}}(L'_{i,n})$ by Lemma 4.3, where $L'_{i,n}$ is given in (16). Note that the diameter $\mathrm{diam}(L'_{i,n}) \simeq 1$. Let $\phi : L'_{i,n} \to [0, 1]$ be a smooth cut-off function that is equal to 0 in a neighborhood of $v_i$, but is equal to 1 at all the other nodal points in $L'_{i,n}$. We introduce the auxiliary function $v = \phi u'$ on $L'_{i,n}$. Consequently, we have for $m \geq 0$ and $1 < p \leq \infty$,

$$\|v\|_{\mathcal{K}^{m,p}_{\vec{1}}(L'_{i,n})} = \|\phi u'\|_{\mathcal{K}^{m,p}_{\vec{1}}(L'_{i,n})} \leq C\|u'\|_{\mathcal{K}^{m,p}_{\vec{1}}(L'_{i,n})}, \tag{20}$$

where $C$ depends on $m$ and the choice of the nodal points. Moreover, since $u(v_i) = 0$, by the definition of $v$, the interpolation $v_I = u'_I = (u_I)'$ on $L'_{i,n}$.

Note that the $\mathcal{K}^{m,p}_{\vec{1}}$ norm and the $W^m_p$ norm are equivalent for $v$ on $L'_{i,n}$, since $v = 0$ in the neighborhood of the vertex $v_i$. Then, by the usual dilation argument in Sobolev spaces, (20), Lemma 4.1, (3), Lemma 4.3, and (14), for $1 < p < \infty$, we have

$$\begin{aligned}
\|u - u_I\|^p_{W^1_p(L_{i,n})} &\leq \kappa_i^{n(2-p)}\|u' - u'_I\|^p_{W^1_p(L'_{i,n})} = \kappa_i^{n(2-p)}\|u' - v + v - u'_I\|^p_{W^1_p(L'_{i,n})} \\
&\leq \kappa_i^{n(2-p)}\left(\|u' - v\|_{W^1_p(L'_{i,n})} + \|v - u'_I\|_{W^1_p(L'_{i,n})}\right)^p \\
&\leq C\kappa_i^{n(2-p)}\left(\|u' - v\|_{\mathcal{K}^{1,p}_{\vec{1}}(L'_{i,n})} + \|v - v_I\|_{W^1_p(L'_{i,n})}\right)^p \\
&\leq C\kappa_i^{n(2-p)}\left(\|u'\|_{\mathcal{K}^{1,p}_{\vec{1}}(L'_{i,n})} + \|v\|_{\mathcal{K}^{k+1,p}_{\vec{1}}(L'_{i,n})}\right)^p \leq C\kappa_i^{n(2-p)}\|u'\|^p_{\mathcal{K}^{k+1,p}_{\vec{1}}(L'_{i,n})} \\
&\leq C\|u\|^p_{\mathcal{K}^{k+1,p}_{\vec{1}}(L_{i,n})} \leq C\kappa_i^{pna_i}\|u\|^p_{\mathcal{K}^{k+1,p}_{\vec{a}+\vec{1}}(L_{i,n})}.
\end{aligned}$$

For $p = \infty$, by the usual dilation argument in Sobolev spaces, (20), Lemma 4.1, (3), Lemma 4.3, and (14), we similarly have

$$\begin{aligned}
\|u - u_I\|_{W^1_\infty(L_{i,n})} &\leq \kappa_i^{-n}\|u' - u'_I\|_{W^1_\infty(L'_{i,n})} = \kappa_i^{-n}\|u' - v + v - u'_I\|_{W^1_\infty(L'_{i,n})} \\
&\leq \kappa_i^{-n}\left(\|u' - v\|_{W^1_\infty(L'_{i,n})} + \|v - u'_I\|_{W^1_\infty(L'_{i,n})}\right) \\
&\leq C\kappa_i^{-n}\left(\|u' - v\|_{\mathcal{K}^{1,\infty}_{\vec{1}}(L'_{i,n})} + \|v - v_I\|_{W^1_\infty(L'_{i,n})}\right) \\
&\leq C\kappa_i^{-n}\left(\|u'\|_{\mathcal{K}^{1,\infty}_{\vec{1}}(L'_{i,n})} + \|v\|_{\mathcal{K}^{k+1,\infty}_{\vec{1}}(L'_{i,n})}\right) \leq C\kappa_i^{-n}\|u'\|_{\mathcal{K}^{k+1,\infty}_{\vec{1}}(L'_{i,n})} \\
&\leq C\|u\|_{\mathcal{K}^{k+1,\infty}_{\vec{1}}(L_{i,n})} \leq C\kappa_i^{na_i}\|u\|_{\mathcal{K}^{k+1,\infty}_{\vec{a}+\vec{1}}(L_{i,n})}.
\end{aligned}$$

Thus, the proof is completed. □

Based on these estimates, we are able to give the range of the grading parameter $\vec{\kappa}$, for which we obtain the optimal convergence rate for the finite element solution $u_n$ approximating Eq. (1) in the $W^1_p$ norm.

**Theorem 4.6.** *Recall the parameters $\sigma$, $a_i$, and $\eta_i$ from Proposition 2.6 for $1 < p < \infty$ and from Proposition 2.7 for $p = \infty$, where $1 \leq i \leq l$. Suppose for some $0 < a_i < \eta_i$, the function $f \in \mathcal{K}^{0,2}_{-\vec{1}}(\Omega) \cap \mathcal{K}^{k-1,p}_{\vec{a}-\vec{1}}(\Omega)$ for $1 < p < \infty$ or $f \in \mathcal{H}^{k-1,\sigma}_{\vec{a}-\vec{1}}(\Omega)$ for $p = \infty$. For the finite element space $S_n$ of degree $k \geq 1$, choose $\kappa_i = \min(2^{-k/a_i}, 1/2)$ in Definition 3.1. Then, for $n$ sufficiently large, the finite element solution $u_n \in S_n$ of Eq. (1) satisfies*

$$\|u - u_n\|_{W^1_p(\Omega)} \leq C\,\mathrm{dim}(S_n)^{-k/2}\|f\|_{\mathcal{K}^{k-1,p}_{\vec{a}-\vec{1}}(\Omega)}, \quad 1 < p < \infty; \tag{21}$$

$$\|u - u_n\|_{W^1_\infty(\Omega)} \leq C\,\mathrm{dim}(S_n)^{-k/2}\|f\|_{\mathcal{H}^{k-1,\sigma}_{\vec{a}-\vec{1}}(\Omega)}, \tag{22}$$

*where $C$ is independent of $n$ and $f$.*

**Proof.** We first show the case for the interpolate error with $1 < p < \infty$. Summing up the estimates in Lemmas 4.2, 4.4, and 4.5 for different sub-regions of the domain $\Omega$, and using the fact that $\kappa_i \le 2^{-k/a_i}$, we have

$$\begin{aligned}\|u-u_I\|^p_{W^1_p(\Omega)} &\le C\Big(2^{-pnk}\|u\|^p_{\mathcal{K}^{k+1,p}_{\vec{a}+\vec{1}}(\Omega_0)} + \sum_{1\le i\le l, 0\le j\le n} \kappa_i^{pja_i} 2^{pk(j-n)}\|u\|^p_{\mathcal{K}^{k+1,p}_{\vec{a}+\vec{1}}(L_{i,j})}\Big)\\ &\le C\Big(2^{-pnk}\|u\|^p_{\mathcal{K}^{k+1,p}_{\vec{a}+\vec{1}}(\Omega_0)} + \sum_{1\le i\le l, 0\le j\le n} 2^{-pkn}\|u\|^p_{\mathcal{K}^{k+1,p}_{\vec{a}+\vec{1}}(L_{i,j})}\Big) \le C2^{-pnk}\|u\|^p_{\mathcal{K}^{k+1,p}_{\vec{a}+\vec{1}}(\Omega)}.\end{aligned}$$

Now, for $p = \infty$, a similar estimate gives

$$\begin{aligned}\|u-u_I\|_{W^1_\infty(\Omega)} &= \max_{1\le i\le l, 0\le j\le n}(\|u-u_I\|_{W^1_\infty(\Omega_0)}, \|u-u_I\|_{W^1_\infty(L_{i,j})})\\ &\le C \max_{1\le i\le l, 0\le j\le n}\Big(2^{-nk}\|u\|_{\mathcal{K}^{k+1,\infty}_{\vec{a}+\vec{1}}(\Omega_0)}, \kappa_i^{ja_i}2^{k(j-n)}\|u\|_{\mathcal{K}^{k+1,\infty}_{\vec{a}+\vec{1}}(L_{i,j})}\Big)\\ &\le C \max_{1\le i\le l, 0\le j\le n}\Big(2^{-nk}\|u\|_{\mathcal{K}^{k+1,\infty}_{\vec{a}+\vec{1}}(\Omega_0)}, 2^{-kn}\|u\|_{\mathcal{K}^{k+1,\infty}_{\vec{a}+\vec{1}}(L_{i,j})}\Big) \le C2^{-nk}\|u\|_{\mathcal{K}^{k+1,\infty}_{\vec{a}+\vec{1}}(\Omega)}.\end{aligned}$$

Recall $\dim(S_n) \simeq 4^n$. Therefore, by (10) in Corollary 3.5 and Proposition 2.6, for $1 < p < \infty$, we have

$$\|u-u_n\|_{W^1_p(\Omega)} \le C\|u-u_I\|_{W^1_p(\Omega)} \le C2^{-nk}\|u\|_{\mathcal{K}^{k+1,p}_{\vec{a}+\vec{1}}(\Omega)} \le C\dim(S_n)^{-k/2}\|f\|_{\mathcal{K}^{k-1,p}_{\vec{a}-\vec{1}}(\Omega)},$$

which proves (21). For $p = \infty$, by (10) and Corollary 2.8, we show (22) by

$$\|u-u_n\|_{W^1_\infty(\Omega)} \le C\|u-u_I\|_{W^1_\infty(\Omega)} \le C2^{-nk}\|u\|_{\mathcal{K}^{k+1,\infty}_{\vec{a}+\vec{1}}(\Omega)} \le C\dim(S_n)^{-k/2}\|f\|_{\mathcal{H}^{k-1,\sigma}_{\vec{a}-\vec{1}}(\Omega)}. \quad \square$$

**Remark 4.7.** Theorem 4.6 gives the range for the grading parameter $\vec{\kappa}$ and the explicit conditions on the right hand side function $f$, such that the optimal convergence rate can be obtained for the finite element solution in the $W^1_p$ norm $(1 < p \le \infty)$ on convex polygonal domains. The ingredients for the $W^1_p$ estimates in Theorem 4.6 are the stability result in Theorem 3.4 and the interpolation error estimate developed in this section. Note that the interpolation error estimates are independent of the convexity of the domain. Therefore, we expect to derive the analogue of Theorem 4.6 for non-convex domains once the stability of the Ritz projection (Theorem 3.4) is available for non-convex domains. This is for the time being still an open problem.

**Remark 4.8.** Define the sign function of a real number $t$

$$\mathrm{sign}(t) = \begin{cases} -1 & \text{if } t < 0,\\ 0 & \text{if } t = 0,\\ 1 & \text{if } t > 0.\end{cases}$$

Then, using the duality argument, the following $L^p$ error estimates can be derived on the graded meshes (see [13,17])

$$\|u-u_n\|^p_{L^p(\Omega)} \le C\big(\inf_{z_1\in S_n}\|u-z_1\|_{W^1_p(\Omega)}\big)\big(\inf_{z_2\in S_n}\|w-z_2\|_{W^1_q(\Omega)}\big), \tag{23}$$

where $1 < p < \infty$, $q = p/(p-1)$, and $w \in W^1_q(\Omega) \cap \{w|_{\partial\Omega} = 0\}$ is the solution to

$$-\Delta w = \mathrm{sign}(u-u_n)|u-u_n|^{p-1} \quad \text{in } \Omega.$$

However, numerical experiments have shown that the actual convergence rate in $L^p$ may be better than that given in (23). A thorough theoretical investigation is thus needed to address this issue and to obtain a sharp $L^p$ error analysis on graded meshes.

## 5. Numerical illustrations

In this section, we report numerical results that confirm our theoretical results in Theorem 4.6. The model problem we shall solve is as follows:

$$-\Delta u = f \quad \text{in } \Omega, \qquad u = 0 \quad \text{on } \partial\Omega, \tag{24}$$

where we choose $f = 1$ and $\Omega$ is a convex polygonal domain. In the numerical tests, we use the linear Lagrange finite element methods associated with the proposed graded meshes.

For the domain $\Omega$ in Eq. (24), denote by $\chi_i$ the interior angle of the domain at the vertex $v_i$. Let $\omega_i \subset \Omega$ be the neighborhood of $v_i$ such that $\bar{\omega}_i$ does not include other vertices. Then, by the regularity estimates in [29], the solution $u|_{\omega_i} \in H^{1+\pi/\chi_i-\epsilon}(\omega_i)$ for $\epsilon > 0$ arbitrarily small. Therefore, when $\chi_i < 90°$, by the Sobolev embedding Theorem, the solution is in $W^2_p$ in the neighborhood $\omega_i$ for any $1 < p \le \infty$. Thus, quasi-uniform meshes near these vertices will lead

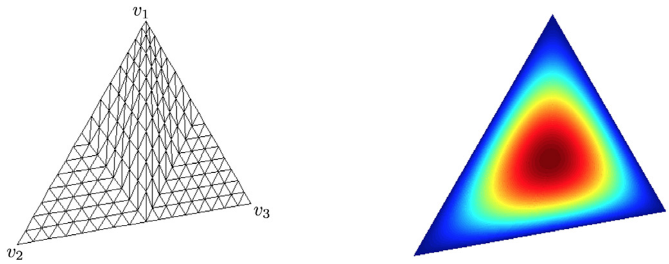


**Fig. 3.** The triangular domain with angles 50°, 60°, and 70°: the graded mesh after three refinements with $\vec{\kappa} = (0.4, 0.5, 0.5)$ (left); the numerical solution (right).

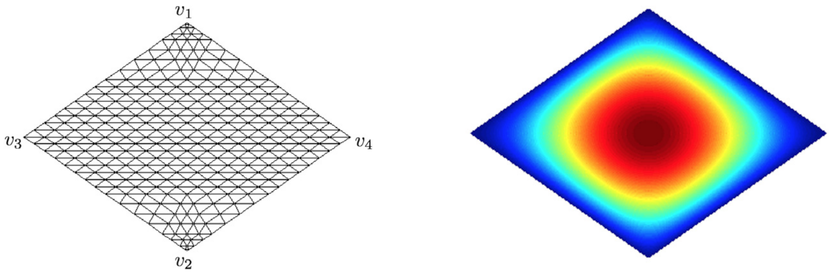


**Fig. 4.** The quadrilateral domain with angles 110° ($v_1$), 110° ($v_2$), 70° ($v_3$), and 70° ($v_4$): the graded mesh after three refinements with $\vec{\kappa} = (0.3, 0.3, 0.5, 0.5)$ (left); the numerical solution (right).

to the first order convergence for the linear approximation. Since the solution is smooth in the interior of the domain, we need to focus on the vertices with angles $>90°$, where special mesh grading may be needed. For these vertices, the optimal graded meshes are determined as follows.

Case I ($1 < p < \infty$). Since $f = 1$ and $\chi_i > 90°$, near $v_i$, $u$ may not belong to $W_p^2$, but $u \in \mathcal{K}^{2,p}_{\vec{a}+\vec{1}}$ for any $0 \le a_i < \eta_i = \pi/\chi_i - 1 + 2/p$ (Proposition 2.6). Based on Theorem 4.6, we can choose the grading parameter for the vertex $v_i$

$$\kappa_i = \min(2^{-1/a_i}, 1/2) \quad \text{for any } 0 < a_i < \eta_i = \pi/\chi_i - 1 + 2/p \tag{25}$$

in order to obtain the optimal convergence rate in the $W_p^1$ norm for the linear finite element solution.

Case II ($p = \infty$). By Proposition 2.7 and Corollary 2.8, near the vertex $v_i$, the solution belongs to $\mathcal{K}^{2,\infty}_{\vec{a}+\vec{1}}$ for any $0 \le a_i < \eta_i$, where the parameter $\eta_i = \pi/\chi_i - 1 - \sigma$. Taking $\sigma \to 0$ and by Theorem 4.6, we can choose the grading parameter for the vertex $v_i$

$$\kappa_i = \min(2^{-1/a_i}, 1/2) \quad \text{for any } 0 < a_i < \eta_i = \pi/\chi_i - 1 \tag{26}$$

in order to obtain the optimal convergence rate in the $W_\infty^1$ norm for the linear finite element solution.

Throughout this section, the convergence rate is computed by taking the ratio of the difference of two consecutive levels. Namely,

$$W_p^1 \text{ convergence rate at level } j := \log_2\left(\frac{\|u_j - u_{j-1}\|_{W_p^1(\Omega)}}{\|u_{j+1} - u_j\|_{W_p^1(\Omega)}}\right). \tag{27}$$

Since the solution $u$ in the model problem is unknown, by Theorem 4.6, the rate in (27) is a good estimation of the actual convergence rate. Recall the dimension of the finite element space $\dim(S_n) \simeq 4^n$. Therefore, we achieve the optimal convergence rate for the linear finite element method when the values computed in (27) converge to 1 as $j$ increases, while we lose the optimal rate if the values from (27) are less than 1. In fact, the closer these values to 1, the better convergence rate we obtain.

To compute the asymptotic convergence rate (27) at the $j$th level, we must compute the difference between functions defined on different grids, one of which is defined on a coarse grid and the other of which is defined on the fine grid. Under the algorithmic strategy that generates the graded mesh, the coarse grid is constructed in such a way that it is nested in the fine grid (see Fig. 2). Therefore, any node in the fine grid is either the node on the coarse grid or it is the point on the edge of the coarse grid triangulation. Therefore, we only need to compute the interpolation of the coarse grid function $u_{j-1}$ onto the fine grid. This can be done using a simple linear interpolation using the patch information of the fine nodes.

To verify the theory in Theorem 4.6, we have tested a variety of domains and graded meshes. These include a triangular domain with acute angles (Fig. 3), various polygonal domains with the largest opening angles ranging from 110° to 150° (Figs. 4–6). For each domain, we report the $W_p^1$ convergence rates (27) on graded meshes $\mathcal{T}_j$ obtained from consecutive

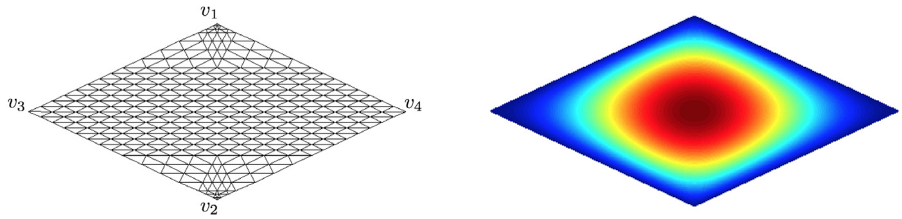


**Fig. 5.** The polygonal domain with angles 130° ($v_1$), 130° ($v_2$), 50° ($v_3$), and 50° ($v_4$): the graded mesh after three refinements with $\vec{\kappa} = (0.2, 0.2, 0.5, 0.5)$ (left); the numerical solution (right).

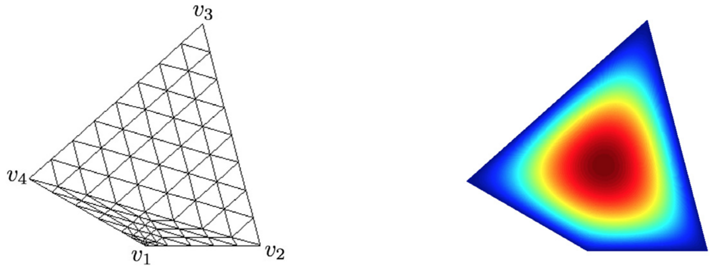


**Fig. 6.** The polygonal domain with angles = 150° at $v_1$, and <90° at other vertices: the graded mesh after three refinements with $\vec{\kappa} = (0.2, 0.5, 0.5, 0.5)$ (left); the numerical solution (right).

**Table 1**
The $W_p^1$ convergence rate of the linear finite element method on the triangular domain (Fig. 3) with $\kappa_1 = 0.4$ and $\kappa_1 = 0.5$.

| $W_p^1$ | $p = 3$ | | $p = 5$ | | $p = 10$ | | $p = 15$ | | $p = \infty$ | |
|---|---|---|---|---|---|---|---|---|---|---|
| $j/\kappa_1$ | 0.4 | 0.5 | 0.4 | 0.5 | 0.4 | 0.5 | 0.4 | 0.5 | 0.4 | 0.5 |
| 6 | 1.00 | 1.00 | 1.00 | 1.00 | 1.00 | 1.00 | 1.00 | 0.99 | 0.95 | 0.96 |
| 7 | 1.00 | 1.00 | 1.00 | 1.00 | 1.00 | 1.00 | 1.00 | 1.00 | 0.98 | 0.98 |
| 8 | 1.00 | 1.00 | 1.00 | 1.00 | 1.00 | 1.00 | 1.00 | 1.00 | 0.99 | 0.99 |
| 9 | 1.00 | 1.00 | 1.00 | 1.00 | 1.00 | 1.00 | 1.00 | 1.00 | 1.00 | 1.00 |
| 10 | 1.00 | 1.00 | 1.00 | 1.00 | 1.00 | 1.00 | 1.00 | 1.00 | 1.00 | 1.00 |

refinements with different parameters $\vec{\kappa}$. We also select different values of $p$ in the range $1 < p \leq \infty$ in these experiments for fully validating our finite element algorithms. The numerical results are listed in Tables 1–4. Note that the parameter $\vec{\kappa}$ controls the mesh refinements near each vertex $v_i$ by the value of $\kappa_i$. As discussed above, we shall use quasi-uniform refinements ($\kappa_i = 0.5$) near vertices with interior angles <90° in all the tests, since it is sufficiently effective approximating local solutions. Thus, in these tables, we only specify the values of $\kappa_i$ that correspond to vertices with interior angles >90°, and the unspecified values of $\kappa_i$ by default equal 1/2. We also highlight the results in some of the columns, which indicates that this column is the border line case in terms of the values of $\kappa_i$, below and equal to which the optimal convergence rate is predicted by the theory.

### *5.1. Numerical tests in $W_p^1$ norms*

We proceed to report the test results.

**Test 1: a triangular domain with angles** 50**°,** 60**°, and** 70**°** (Fig. 3). For this case, the solution in fact belongs to $W_p^2(\Omega)$ for $1 < p \leq \infty$. Therefore, for a vertex $v_i$, we can choose any value $\kappa_i \in (0, 1/2]$ to obtain the optimal convergence in the $W_p^1$ norm. In particular, quasi-uniform refinements should lead to the optimal convergence rate. We, therefore, report the convergence history only for two values of $\vec{\kappa}$: (I) $\vec{\kappa} = (0.4, 0.5, 0.5)$; (II) $\vec{\kappa} = (0.5, 0.5, 0.5)$ (quasi-uniform refinements). The $W_p^1$ convergence rates for $p = 3, 5, 10, 15$, and $\infty$ in Table 1 verify this theoretical prediction. A sample mesh and the numerical solution are presented in Fig. 3.

**Test 2: a polygonal domain with the largest opening angle** 110**°** (Fig. 4). As mentioned above, we choose $\kappa_3 = \kappa_4 = 0.5$ for the vertices $v_3$ and $v_4$ due to the angle condition. In view of (25) and (26), for the vertices $v_1$ and $v_2$, since $\pi/\chi_i = 18/11$ ($i = 1, 2$), special mesh grading may be necessary. In particular, for $1 < p < \infty$, we can choose

$$\kappa_i = \min(2^{-1/a_i}, 1/2) \quad \text{for any } 0 < a_i < 18/11 - 1 + 2/p = 7/11 + 2/p;$$

and for $p = \infty$, we choose

$$\kappa_i = 2^{-1/a_i} \quad \text{for any } 0 < a_i < 18/11 - 1 = 7/11.$$

**Table 2**
The $W_p^1$ convergence rate of the linear finite element method for $p = 3, 5, 10, 15$ and $p = \infty$ on the polygonal domain with the 110° angles (Fig. 4).

| $W_p^1$ | $p=3$ | | | | | $p=5$ | | | | |
|---|---|---|---|---|---|---|---|---|---|---|
| $j/\kappa_1=\kappa_2$ | 0.1 | 0.2 | 0.3 | 0.4 | 0.5 | 0.1 | 0.2 | 0.3 | 0.4 | 0.5 |
| 6 | 1.01 | 1.01 | 1.01 | 1.01 | 0.99 | 0.99 | 1.00 | 1.00 | 1.02 | 0.90 |
| 7 | 1.01 | 1.01 | 1.01 | 1.01 | 0.99 | 1.00 | 1.00 | 1.00 | 1.01 | 0.92 |
| 8 | 1.00 | 1.00 | 1.00 | 1.00 | 1.00 | 1.00 | 1.00 | 1.00 | 1.00 | 0.93 |
| 9 | 1.00 | 1.00 | 1.00 | 1.00 | 1.00 | 1.00 | 1.00 | 1.00 | 1.00 | 0.95 |
| 10 | 1.00 | 1.00 | 1.00 | 1.00 | 1.00 | 1.00 | 1.00 | 1.00 | 1.00 | 0.96 |

| $W_p^1$ | $p=10$ | | | | | $p=15$ | | | | |
|---|---|---|---|---|---|---|---|---|---|---|
| $j/\kappa_1=\kappa_2$ | 0.1 | 0.2 | 0.3 | 0.4 | 0.5 | 0.1 | 0.2 | 0.3 | 0.4 | 0.5 |
| 6 | 0.96 | 0.99 | 0.99 | 1.00 | 0.74 | 0.94 | 0.99 | 0.98 | 0.94 | 0.68 |
| 7 | 0.99 | 1.00 | 1.00 | 1.01 | 0.77 | 0.98 | 1.00 | 0.99 | 0.96 | 0.70 |
| 8 | 1.00 | 1.00 | 1.00 | 1.01 | 0.78 | 0.99 | 1.00 | 1.00 | 0.97 | 0.72 |
| 9 | 1.00 | 1.00 | 1.00 | 1.00 | 0.79 | 1.00 | 1.00 | 1.00 | 0.98 | 0.73 |
| 10 | 1.00 | 1.00 | 1.00 | 1.00 | 0.80 | 1.00 | 1.00 | 1.00 | 0.99 | 0.74 |

| $W_p^1$ | $p=\infty$ | | | | |
|---|---|---|---|---|---|
| $j/\kappa_1=\kappa_2$ | 0.1 | 0.2 | 0.3 | 0.4 | 0.5 |
| 6 | 0.89 | 0.90 | 0.91 | 0.76 | 0.55 |
| 7 | 0.88 | 0.94 | 0.94 | 0.79 | 0.57 |
| 8 | 0.94 | 0.96 | 0.96 | 0.80 | 0.59 |
| 9 | 0.97 | 0.97 | 0.97 | 0.81 | 0.60 |
| 10 | 0.98 | 0.98 | 0.98 | 0.82 | 0.61 |

Therefore, for the first two vertices ($i = 1, 2$), the optimal ranges for some specific values of $p$ are:

$$\begin{cases} \kappa_i \in (0, 0.5]\ (p=3), \quad \kappa_i \in (0, 0.5]\ (p=5), \quad \kappa_i \in (0, 0.436)\ (p=10), \\ \kappa_i \in (0, 0.406)\ (p=15), \quad \kappa_i \in (0, 0.336)\ (p=\infty). \end{cases} \tag{28}$$

In Table 2, we list the convergence rates of the numerical solutions on meshes with $\kappa_1 = \kappa_2 = 0.1 - 0.5$ (recall that $\kappa_3 = \kappa_4 = 0.5$ for all the meshes). It is clear from the table that for $p = 3$ and 5, the optimal convergence rate is achieved for all $\kappa_1, \kappa_2 \le 0.5$; for $p = 10$ and 15, we obtain the optimal convergence rate when $\kappa_1, \kappa_2 \le 0.4$ but lose the optimal rate on quasi-uniform meshes $\kappa_1 = \kappa_2 = 0.5$; for $p = \infty$, the optimal rate is obtained when $\kappa \le 0.3$ but not when $\kappa = 0.4$ and 0.5. These numerical results verify the theoretical prediction. Namely, our construction (28) leads to finite element methods that approximate the solution with the optimal convergence rate in the $W_p^1$ norm. A sample mesh is demonstrated in Fig. 4.

**Test 3: a polygonal domains with the largest opening angle** 130° (Fig. 5). For this case, the optimal range for the parameter $\vec{\kappa}$ is determined as follows. For the vertices $v_3$ and $v_4$, it is sufficient to choose $\kappa_3 = \kappa_4 = 0.5$ for all the values of $p$, since $\chi_i < 90°$. For the vertices $v_1$ and $v_2$, since $\pi/\chi_i = 18/13$ $(i = 1, 2)$, special mesh grading may be necessary to obtain the optimal convergence rate. In view of (25) and (26), for $1 < p < \infty$, we can choose

$$\kappa_i = \min(2^{-1/a_i}, 1/2) \quad \text{for any } 0 < a_i < 18/13 - 1 + 2/p = 5/13 + 2/p;$$

and for $p = \infty$, we choose

$$\kappa_i = 2^{-1/a_i} \quad \text{for any } 0 < a_i < 18/13 - 1 = 5/13.$$

Thus, by Theorem 4.6, for the first two vertices ($i = 1, 2$), the optimal ranges for some specific values of $p$ are:

$$\begin{cases} \kappa_i \in (0, 0.5]\ (p=15/14), \quad \kappa_i \in (0, 0.5]\ (p=3), \quad \kappa_i \in (0, 0.413)\ (p=5), \\ \kappa_i \in (0, 0.305)\ (p=10), \quad \kappa_i \in (0, 0.262)\ (p=15), \quad \kappa_i \in (0, 0.164)\ (p=\infty). \end{cases} \tag{29}$$

In Table 3, we list the convergence rates of the numerical solutions on meshes with $\kappa_1 = \kappa_2 = 0.1 - 0.5$ (recall that $\kappa_3 = \kappa_4 = 0.5$ for all the meshes). These results, similar to those in Test 2, illustrate the effectiveness of our algorithms in (29) to recover the optimal rate of convergence in the $W_p^1$ norm for $1 < p \le \infty$.

**Test 4: a polygonal domain with the largest opening angle** 150° (Fig. 6). The fourth set of tests are performed on a polygonal domain with the largest corner angle given by 150° at the vertex $v_1$. We choose the domain such that the interior angles at other vertices are less than 90°. Thus, we only need to focus on possible special refinements near $v_1$, since quasi-uniform refinements ($\kappa_i = 0.5$) near other vertices shall be sufficient for good linear finite element approximations in $W_p^1$ for $1 < p \le \infty$.

As in Test 2 and Test 3, the optimal range of the grading parameter $\kappa_1$ at the vertex $v_1$ depends on the index $p$ of the $W_p^1$ space. In particular, for $1 < p < \infty$, by (25), we can choose

$$\kappa_1 = \min(2^{-1/a_1}, 1/2) \quad \text{for any } 0 < a_1 < 18/15 - 1 + 2/p = 1/5 + 2/p.$$

**Table 3**
The $W_p^1$ convergence rate of the linear finite element method for $p = 15/14, 3, 5, 10, 15$ and $p = \infty$ on the polygonal domain with 130° angles (Fig. 5).

| $W_p^1$ | $p = 15/14$ | | | | | $p = 3$ | | | | |
|---|---|---|---|---|---|---|---|---|---|---|
| $j/\kappa_1 = \kappa_2$ | 0.1 | 0.2 | 0.3 | 0.4 | 0.5 | 0.1 | 0.2 | 0.3 | 0.4 | 0.5 |
| 6 | 1.01 | 1.01 | 1.01 | 1.01 | 1.01 | 1.00 | 1.01 | 1.01 | 1.00 | 0.91 |
| 7 | 1.01 | 1.01 | 1.01 | 1.01 | 1.01 | 1.00 | 1.01 | 1.01 | 1.01 | 0.93 |
| 8 | 1.00 | 1.00 | 1.00 | 1.00 | 1.01 | 1.00 | 1.00 | 1.00 | 1.00 | 0.94 |
| 9 | 1.00 | 1.00 | 1.00 | 1.00 | 1.00 | 1.00 | 1.00 | 1.00 | 1.00 | 0.95 |
| 10 | 1.00 | 1.00 | 1.00 | 1.00 | 1.00 | 1.00 | 1.00 | 1.00 | 1.00 | 0.96 |
| $W_p^1$ | $p = 5$ | | | | | $p = 10$ | | | | |
| $j/\kappa_1 = \kappa_2$ | 0.1 | 0.2 | 0.3 | 0.4 | 0.5 | 0.1 | 0.2 | 0.3 | 0.4 | 0.5 |
| 6 | 0.98 | 1.00 | 1.01 | 0.96 | 0.73 | 0.91 | 0.98 | 0.99 | 0.74 | 0.54 |
| 7 | 1.00 | 1.00 | 1.00 | 0.97 | 0.75 | 0.96 | 0.99 | 1.00 | 0.76 | 0.56 |
| 8 | 1.00 | 1.00 | 1.00 | 0.98 | 0.76 | 0.99 | 1.00 | 1.00 | 0.76 | 0.57 |
| 9 | 1.00 | 1.00 | 1.00 | 0.98 | 0.77 | 1.00 | 1.00 | 0.99 | 0.77 | 0.57 |
| 10 | 1.00 | 1.00 | 1.00 | 0.98 | 0.77 | 1.00 | 1.00 | 0.99 | 0.77 | 0.58 |
| $W_p^1$ | $p = 15$ | | | | | $p = \infty$ | | | | |
| $j/\kappa_1 = \kappa_2$ | 0.1 | 0.2 | 0.3 | 0.4 | 0.5 | 0.1 | 0.2 | 0.3 | 0.4 | 0.5 |
| 6 | 0.87 | 0.93 | 0.89 | 0.65 | 0.48 | 0.76 | 0.89 | 0.65 | 0.48 | 0.34 |
| 7 | 0.94 | 0.95 | 0.89 | 0.67 | 0.49 | 0.87 | 0.89 | 0.66 | 0.49 | 0.36 |
| 8 | 0.98 | 0.98 | 0.90 | 0.67 | 0.50 | 0.93 | 0.89 | 0.66 | 0.50 | 0.37 |
| 9 | 0.99 | 0.99 | 0.90 | 0.68 | 0.51 | 0.96 | 0.89 | 0.67 | 0.50 | 0.37 |
| 10 | 1.00 | 1.00 | 0.90 | 0.68 | 0.51 | 0.98 | 0.89 | 0.67 | 0.51 | 0.38 |

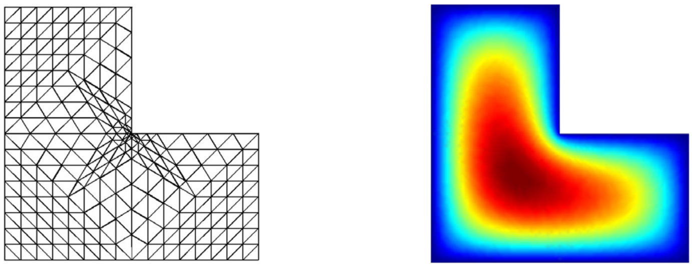

**Fig. 7.** The L-shaped domain: the graded mesh after three refinements with $\kappa_1 = 0.2$ toward the reentrant corner (left); the numerical solution (right).

Thus, by Theorem 4.6, for the vertex $v_1$, the optimal ranges for some specific values of $p$ are:

$$\begin{cases} \kappa_1 \in (0, 0.5]\ (p = 15/14), \quad \kappa_1 \in (0, 0.449]\ (p = 3), \quad \kappa_1 \in (0, 0.315)\ (p = 5), \\ \kappa_1 \in (0, 0.176)\ (p = 10), \quad \kappa_1 \in (0, 0.125)\ (p = 15). \end{cases} \tag{30}$$

The convergence rates of the numerical solutions on meshes with $\kappa_1 = 0.1 - 0.5$ are listed in Table 4. It is evident from this table that for any test value of $p$, we obtain optimal convergence rates when the grading parameter stays within the range given in (30); and we lose the optimal rate for any value of $\kappa_1$ that is out of the range. This implies that sufficient mesh grading is necessary to achieve the optimal convergence rate in $W_p^1$ when approximating singular solutions. The theory that leads to the sharp selection criteria for the grading parameters is once again clearly verified.

### *5.2. Additional numerical results*

Recall the hypothesis in Remark 4.7 for the $W_p^1$ convergence on non-convex domains and the claims in Remark 4.8 for the $L^p$ convergence on convex domains. We here report some corresponding numerical results for readers' reference.

In Table 5, we display the $W_p^1$ convergence rate of the numerical solution on a non-convex domain (the L-shaped domain in Fig. 7). Let $v_1$ be the vertex associated with the reentrant corner. In view of (25), near other vertices, quasi-uniform meshes are sufficient for the optimal $W_p^1$ convergence with the selected values of $p$. Therefore, we only test different values of the grading parameter $\kappa_1$ for the vertex $v_1$. Although our theoretical results do not apply to non-convex domains, the numerical tests seem to imply that the formula (25) still gives rise to the optimal convergence rate in these $W_p^1$ norms. For example, using (25), we have the ranges of $\kappa_1$ near $v_1$

$$\kappa_1 \in (0, 0.5]\ (p = 15/14) \quad \text{and} \quad \kappa_1 \in (0, 0.125)\ (p = 3),$$

which are consistent with the ranges in Table 5, for which the optimal $W_p^1$ convergence is obtained.

**Table 4**
The $W_p^1$ convergence rate of the linear finite element method for $p = 15/14, 3, 5, 10$, and 15 on the polygonal domain with a 150° angle (Fig. 6).

| $W_p^1$ | $p = 15/14$ | | | | | $p = 3$ | | | | |
|---|---|---|---|---|---|---|---|---|---|---|
| $j/\kappa_1$ | 0.1 | 0.2 | 0.3 | 0.4 | 0.5 | 0.1 | 0.2 | 0.3 | 0.4 | 0.5 |
| 6 | 1.01 | 1.01 | 1.01 | 1.02 | 1.01 | 1.02 | 1.02 | 1.02 | 1.01 | 0.89 |
| 7 | 1.01 | 1.01 | 1.01 | 1.01 | 1.01 | 1.01 | 1.01 | 1.00 | 1.01 | 0.87 |
| 8 | 1.00 | 1.00 | 1.00 | 1.00 | 1.01 | 1.01 | 1.01 | 1.01 | 1.00 | 0.87 |
| 9 | 1.00 | 1.00 | 1.00 | 1.00 | 1.00 | 1.00 | 1.00 | 1.00 | 1.00 | 0.87 |
| 10 | 1.00 | 1.00 | 1.00 | 1.00 | 1.00 | 1.00 | 1.00 | 1.00 | 1.00 | 0.86 |

| $W_p^1$ | $p = 5$ | | | | |
|---|---|---|---|---|---|
| $j/\kappa_1$ | 0.1 | 0.2 | 0.3 | 0.4 | 0.5 |
| 6 | 1.02 | 1.01 | 1.01 | 0.82 | 0.58 |
| 7 | 1.01 | 1.01 | 1.01 | 0.80 | 0.59 |
| 8 | 1.01 | 1.01 | 1.00 | 0.80 | 0.59 |
| 9 | 1.00 | 1.00 | 1.00 | 0.79 | 0.60 |
| 10 | 1.00 | 1.00 | 1.00 | 0.79 | 0.60 |

| $W_p^1$ | $p = 10$ | | | | | $p = 15$ | | | | |
|---|---|---|---|---|---|---|---|---|---|---|
| $j/\kappa_1$ | 0.1 | 0.2 | 0.3 | 0.4 | 0.5 | 0.1 | 0.2 | 0.3 | 0.4 | 0.5 |
| 6 | 0.99 | 0.97 | 0.70 | 0.52 | 0.38 | 0.95 | 0.80 | 0.58 | 0.43 | 0.31 |
| 7 | 1.00 | 0.98 | 0.70 | 0.53 | 0.39 | 0.98 | 0.78 | 0.58 | 0.44 | 0.32 |
| 8 | 1.00 | 0.98 | 0.70 | 0.53 | 0.39 | 0.99 | 0.78 | 0.58 | 0.44 | 0.33 |
| 9 | 1.00 | 0.97 | 0.70 | 0.53 | 0.40 | 1.00 | 0.78 | 0.58 | 0.44 | 0.33 |
| 10 | 1.00 | 0.96 | 0.70 | 0.53 | 0.40 | 1.00 | 0.78 | 0.58 | 0.44 | 0.33 |

**Table 5**
The $W_p^1$ convergence rate of the linear finite element method for $p = 15/14$ and 3 on the L-shaped domain (Fig. 7).

| $W_p^1$ | $p = 15/14$ | | | | | $p = 3$ | | | | |
|---|---|---|---|---|---|---|---|---|---|---|
| $j/\kappa_1$ | 0.1 | 0.2 | 0.3 | 0.4 | 0.5 | 0.1 | 0.2 | 0.3 | 0.4 | 0.5 |
| 6 | 1.00 | 1.00 | 1.00 | 1.00 | 1.00 | 0.97 | 0.93 | 0.77 | 0.58 | 0.43 |
| 7 | 1.01 | 1.00 | 1.01 | 1.00 | 1.00 | 0.98 | 0.91 | 0.69 | 0.49 | 0.36 |
| 8 | 1.00 | 1.00 | 1.00 | 1.00 | 1.00 | 0.98 | 0.88 | 0.63 | 0.46 | 0.34 |
| 9 | 1.00 | 1.00 | 1.00 | 1.00 | 1.00 | 0.99 | 0.85 | 0.60 | 0.45 | 0.34 |
| 10 | 1.00 | 1.00 | 1.00 | 1.00 | 1.00 | 0.99 | 0.83 | 0.59 | 0.44 | 0.33 |

**Table 6**
The $L^p$ convergence rate of the linear finite element method for $p = 3$ and 5 on the polygonal domain with a 150° angle (Fig. 6).

| $L^p$ | $p = 3$ | | | | | $p = 5$ | | | | |
|---|---|---|---|---|---|---|---|---|---|---|
| $j/\kappa_1$ | 0.1 | 0.2 | 0.3 | 0.4 | 0.5 | 0.1 | 0.2 | 0.3 | 0.4 | 0.5 |
| 6 | 1.96 | 1.96 | 1.97 | 1.98 | 1.97 | 1.97 | 1.96 | 1.96 | 1.98 | 1.94 |
| 7 | 1.99 | 2.00 | 1.99 | 1.99 | 1.97 | 1.99 | 1.99 | 1.99 | 1.99 | 1.74 |
| 8 | 2.00 | 2.00 | 2.00 | 1.99 | 1.96 | 2.00 | 2.00 | 2.00 | 1.99 | 1.55 |
| 9 | 2.00 | 2.00 | 2.00 | 2.00 | 1.96 | 2.00 | 2.00 | 2.00 | 1.99 | 1.53 |
| 10 | 2.00 | 2.00 | 2.00 | 2.00 | 1.96 | 2.00 | 2.00 | 2.00 | 2.00 | 1.53 |

In Table 6, we list the $L^p$ convergence rate on the polygonal domain (Fig. 6) for the same numerical solutions as in Test 4. Recall that the highlighted columns correspond to the border line case for the values of $\kappa_1$, below and equal to which the optimal $W_p^1$ convergence is predicted by our theory. However, it seems that for $p = 3$ and 5, the $L^p$ convergence rates are optimal for $\kappa_1 \leq 0.5$ and $\kappa_1 \leq 0.4$, respectively. These are better convergence results than those predicted by (23), and imply that the range of the grading parameter for the optimal $L^p$ convergence may be larger than the range of the parameter for the optimal $W_p^1$ convergence.

## 6. Conclusion

We study the regularity and finite element approximations for elliptic equations in the $W_p^1$ norm ($1 < p \leq \infty$), especially when the solution possesses singularities due to the non-smoothness of the domain. Using appropriate weighted Sobolev spaces and weighted Hölder spaces, we first formulate regularity estimates for the singular solution that resemble the full-regularity result for smooth solutions in the usual Sobolev spaces. Then, we describe the construction of a family of graded meshes and the associated finite element methods. We further provide the regularity requirement on the given data and propose specific selection criteria for the grading parameters, such that the associated finite element solution approximates the possible singular solution with the optimal convergence rate in the $W_p^1$ norm. The ingredients of our approach include the regularity estimates in weighted spaces (Propositions 2.6, 2.7 and Corollary 2.8), a finite element stability result on graded meshes (Theorem 3.4), and rigorous interpolation error estimates in weighted spaces. Numerical experiments are conducted on a variety of test problems. The numerical results are clearly aligned with the theoretical prediction, and hence validate the proposed method.

## Acknowledgments

Y.-J. Lee was partially supported by the National Science Foundation (NSF) Grant DMS-1358953. H. Li was partially supported by the NSF Grant DMS-1418853, by the Natural Science Foundation of China (NSFC) Grant 11628104, and by the Wayne State University Grants Plus Program.

## References

[1] S.C. Brenner, L.R. Scott, The Mathematical Theory of Finite Element Methods, second ed., in: Texts in Applied Mathematics, vol. 15, Springer-Verlag, New York, 2002.
[2] P. Ciarlet, The Finite Element Method for Elliptic Problems, in: Studies in Mathematics and Its Applications, vol. 4, North-Holland, Amsterdam, 1978.
[3] T. Apel, A.-M. Sändig, J. Whiteman, Graded mesh refinement and error estimates for finite element solutions of elliptic boundary value problems in non-smooth domains, Math. Methods Appl. Sci. 19 (1) (1996) 63–85.
[4] I. Babuška, R.B. Kellogg, J. Pitkäranta, Direct and inverse error estimates for finite elements with mesh refinements, Numer. Math. 33 (4) (1979) 447–471.
[5] C. Băcuţă, V. Nistor, L.T. Zikatanov, Improving the rate of convergence of 'high order finite elements' on polygons and domains with cusps, Numer. Math. 100 (2) (2005) 165–184.
[6] S.C. Brenner, J. Cui, L.-Y. Sung, Multigrid methods for the symmetric interior penalty method on graded meshes, Numer. Linear Algebra Appl. 16 (6) (2009) 481–501.
[7] H. Li, A. Mazzucato, V. Nistor, Analysis of the finite element method for transmission/mixed boundary value problems on general polygonal domains, Electron. Trans. Numer. Anal. 37 (2010) 41–69.
[8] P. Morin, R. Nochetto, K. Siebert, Convergence of adaptive finite element methods, SIAM Rev. 44 (4) (2003) 631–658. (electronic) 2002. Revised reprint of "Data oscillation and convergence of adaptive FEM" [SIAM J. Numer. Anal. 38 (2000), no. 2, 466–488 (electronic); MR1770058 (2001g:65157)].
[9] G. Raugel, Résolution numérique par une méthode d'éléments finis du problème de Dirichlet pour le laplacien dans un polygone, C. R. Acad. Sci., Paris Sér. A–B 286 (18) (1978) A791–A794.
[10] A. Demlow, Localized pointwise a posteriori error estimates for gradients of piecewise linear finite element approximations to second-order quadilinear elliptic problems, SIAM J. Numer. Anal. 44 (2) (2006) 494–514. (electronic).
[11] A. Demlow, D. Leykekhman, A.H. Schatz, L.B. Wahlbin, Best approximation property in the $W_\infty^1$ norm for finite element methods on graded meshes, Math. Comp. 81 (278) (2012) 743–764.
[12] J. Douglas Jr., T. Dupont, A Galerkin method for a nonlinear Dirichlet problem, Math. Comp. 29 (1975) 689–696.
[13] H. Li, The $W_p^1$ stability of the Ritz projection on graded meshes, Math. Comp. 86 (303) (2017) 49–74.
[14] I. Fried, On the optimality of the pointwise accuracy of the finite element solution, Internat. J. Numer. Methods Engrg. 15 (3) (1980) 451–456.
[15] F. Natterer, Über die punktweise Konvergenz finiter Elemente, Numer. Math. 25 (1) (1975/1976) 67–77.
[16] J. Nitsche, $L_\infty$-convergence of finite element approximations, in: Mathematical Aspects of Finite Element Methods (Proc. Conf., Consiglio Naz. delle Ricerche (C.N.R.), Rome, 1975), in: Lecture Notes in Math., vol. 606, Springer, Berlin, 1977, pp. 261–274.
[17] R. Rannacher, R. Scott, Some optimal error estimates for piecewise linear finite element approximations, Math. Comp. 38 (158) (1982) 437–445.
[18] A.H. Schatz, L.B. Wahlbin, Maximum norm estimates in the finite element method on plane polygonal domains. I, Math. Comp. 32 (141) (1978) 73–109.
[19] A.H. Schatz, L.B. Wahlbin, Maximum norm estimates in the finite element method on plane polygonal domains. II. Refinements, Math. Comp. 33 (146) (1979) 465–492.
[20] R. Scott, Optimal $L^\infty$ estimates for the finite element method on irregular meshes, Math. Comp. 30 (136) (1976) 681–697.
[21] T. Apel, A. Rösch, D. Sirch, $L^\infty$-error estimates on graded meshes with application to optimal control, SIAM J. Control Optim. 48 (3) (2009) 1771–1796.
[22] I. Babuška, J. Osborn, Analysis of finite element methods for second order boundary value problems using mesh dependent norms, Numer. Math. 34 (1) (1980) 41–62.
[23] V. Kozlov, V. Maz'ya, J. Rossmann, Spectral Problems Associated with Corner Singularities of Solutions to Elliptic Equations, in: Mathematical Surveys and Monographs, vol. 85, American Mathematical Society, Providence, RI, 2001.
[24] S. Nazarov, B. Plamenevsky, Elliptic Problems in Domains with Piecewise Smooth Boundaries, in: de Gruyter Expositions in Mathematics, vol. 13, Walter de Gruyter & Co., Berlin, 1994.
[25] A. Buffa, M. Costabel, M. Dauge, Anisotropic regularity results for Laplace and Maxwell operators in a polyhedron, C. R. Math. Acad. Sci. Paris 336 (7) (2003) 565–570.
[26] M. Costabel, M. Dauge, S. Nicaise, Analytic regularity for linear elliptic systems in polygons and polyhedra, Math. Models Methods Appl. Sci. 22 (8) (2012) 1250015. 63.
[27] B. Guo, C. Schwab, Analytic regularity of Stokes flow on polygonal domains in countably weighted Sobolev spaces, J. Comput. Appl. Math. 190 (1–2) (2006) 487–519.
[28] V.A. Kondrat'ev, Boundary value problems for elliptic equations in domains with conical or angular points, Trudy Moskov. Mat. Obšč. 16 (1967) 209–292.
[29] P. Grisvard, Singularities in Boundary Value Problems, in: Research Notes in Applied Mathematics, vol. 22, Springer-Verlag, New York, 1992.
[30] V. Maz'ya, J. Rossmann, Elliptic Equations in Polyhedral Domains, in: Mathematical Surveys and Monographs, vol. 162, American Mathematical Society, Providence, RI, 2010.
[31] D. Gilbarg, N. Trudinger, Elliptic Partial Differential Equations of Second Order, in: Grundlehren der Mathematischen Wissenschaften, vol. 224, Springer-Verlag, Berlin, 1977.
[32] H. Li, V. Nistor, Analysis of a modified Schrödinger operator in 2D: regularity, index, and FEM, J. Comput. Appl. Math. 224 (1) (2009) 320–338.